



Research paper

Discovery of phenyl-linked symmetric small molecules as inhibitors of the programmed cell death-1/programmed cell death-ligand 1 interaction



Yizhe Wu^{a,1}, Yu Zhang^{a,1}, Yu Guo^{a,1}, Zhichao Pan^a, Shichun Zhong^a, Xinxin Jin^a, Weihao Zhuang^a, Sikang Chen^a, Jian Gao^a, Wenhai Huang^b, Xiaowu Dong^{a,c,d}, Jinxin Che^{a,c,*}

^a Hangzhou Institute of Innovative Medicine, Institute of Drug Discovery and Design, College of Pharmaceutical Sciences, Zhejiang University, Hangzhou, 310058, PR China

^b Key Laboratory of Neuropsychiatric Drug Research of Zhejiang Province, Hangzhou Medical College, Hangzhou, 310013, PR China

^c Innovation Institute for Artificial Intelligence in Medicine of Zhejiang University, Hangzhou, 310018, PR China

^d Cancer Center, Zhejiang University, Hangzhou, 310058, PR China

ARTICLE INFO

Article history:

Received 18 April 2021

Received in revised form

1 June 2021

Accepted 5 June 2021

Available online 11 June 2021

Keywords:

Immune checkpoint

PD-1/PD-L1

Phenyl-linker

C₂-symmetric small molecules

PD-1/PD-L1 interaction inhibitors

IFN- γ secretion

ABSTRACT

Programmed cell death-1/programmed cell death ligand 1 (PD-1/PD-L1) is one of the most promising targets in the field of immune checkpoint blockade therapy. Beginning with our exploration of linkers and structure-activity relationship research, we found that the aromatic ring could replace the linker and aryl group to maintain the satisfactory activity of classic triaryl scaffold inhibitor. Based on previous studies, we designed and synthesized a series of C₂-symmetric phenyl-linked compounds, and further tail optimization afforded the inhibitors, which displayed promising inhibitory activity against the PD-1/PD-L1 interaction with IC₅₀ value at the single nanomolar range (**C13**–**C15**). Further cell-based PD-1/PD-L1 blockade bioassays indicated that these C₂-symmetric molecules could significantly inhibit the PD-1/PD-L1 interaction at the cellular level and restore T cells' immune function at the safety concentrations. The discovery of these phenyl-linked symmetric small molecules showed the potential of simplified-linker and C₂-symmetric strategy and provided a basis for developing symmetric small molecule inhibitors of PD-1/PD-L1 interaction. Moreover, **C13** and **C15** performed stable binding modes to PD-L1 dimeric after computational docking and dynamic simulation, which may serve as a good starting point for further development.

© 2021 Elsevier Masson SAS. All rights reserved.

1. Introduction

Immunotherapy has been widely used in the treatment of various cancers as a potential subversive strategy [1]. Cancer immunotherapy, such as cancer vaccines, adoptive T-cell therapy, and immune checkpoint blockade, which aims to fight tumors by stimulating the immune system, has become one of the fastest-growing areas of cancer therapy [2,3]. As an inhibitory pathway in the immune system, immune checkpoints are regulated by the

corresponding ligand/receptor interaction [4,5]. It plays an important role in maintaining self-immune tolerance and regulating the duration and amplitude of physiological immune response so as to avoid damage to normal tissues caused by the immune system [5,6]. Among them, programmed cell death-1/programmed cell death ligand 1 (PD-1/PD-L1) is one of the most promising targets in the field of immune-oncology [7]. PD-1 is mainly expressed in activated T cells and B cells, and its function is to inhibit cell over-activation, which is a normal homeostasis mechanism of the immune system [8]. The tumor microenvironment will induce the infiltrating T cells to overexpress PD-1, while the tumor cells overexpress PD-L1 and PD-L2, leading to the continuous activation of the PD-1 pathway in the tumor microenvironment [8,9]. Therefore, even if T cells recognize tumor cells and the tumor antigen binds to T cell receptors, the function of T cells will be

* Corresponding author. Hangzhou Institute of Innovative Medicine, Institute of Drug Discovery and Design, College of Pharmaceutical Sciences, Zhejiang University, Hangzhou, 310058, PR China.

E-mail address: chejx@zju.edu.cn (J. Che).

¹ These authors contributed equally to this work.

inhibited, thus unable to kill tumor cells.

As an effective way to block protein-protein interaction, several clinical trials of humanized monoclonal antibody (mAb) against PD-1/PD-L1 have shown satisfactory anti-tumor effects [10,11]. In the last decade, six mAbs against PD-1 or PD-L1 (anti-PD-1: nivolumab, pembrolizumab, and cemiplimab; anti-PD-L1: atezolizumab, avelumab, and durvalumab) have been approved by the FDA [12,13]. In addition, many mAbs are still in clinical trials worldwide [13,14]. Notably, PD-1/PD-L1 mAbs have shown significant clinical efficacy in various tumors, including melanoma, lung cancer, Hodgkin's lymphoma, urothelial carcinoma, bladder cancer, and etc., [15–20]. The clinical use of these antibodies has proved that PD-1/PD-L1 are promising targets. However, at present, there is still a lack of small molecule drugs acting by the blockade on PD-1/PD-L1 interaction [21]. As a potential complementary strategy of antibody therapy, the development of small molecule PD-1/PD-L1 blockers has been gradually put on the agenda [22].

Recently, a series of inhibitors, including macrocyclic peptides, peptide analogs, and non-peptide small molecules, have been developed to provide pharmacokinetic (PK) properties, stability, and oral bioavailability different from antibodies [12,21], of which BMS986189 (BMS), CA-170 (Aurigene), INCB086550 (Incyte), IMMH-010 (Chasesun), GS-4224 (Gilead) and MAX-10181 (Maxinovel) have entered clinical trials [7,23]. To date, compounds with triaryl scaffolds are the dominant class of small molecule inhibitors of PD-1/PD-L1 interaction [24]. Bristol Myer Squibb (BMS) is the first company to unveil small molecule inhibitors of PD-1/PD-L1 with triaryl scaffold, such as BMS-202 and BMS-8 (Fig. 1) [25,26]. Incyte corporation retained the biphenyl part and replaced the methylene ether structure with the amide bond (Fig. 1), showing significant inhibitory activity against PD-1/PD-L1 binding with IC₅₀ values in the nanomolar range [27,28]. It is not difficult to find that the small molecule inhibitors with such triaryl scaffold are mostly composed of biarylcore group, aryl group, linker connecting them, and tail [29–31]. Interestingly, as the bridge between the biaryl core and the aryl ring, the linker does not show the key interaction with PD-L1 in some crystal structures and docking models [32–34]. However, the effect of different linkers on the activity of inhibitors is significant, which gives rise to our interest in this part. Moreover, recent studies have shown that a series of C₂-symmetric molecules could induce the dimerization of PD-L1, resulting in an antiparallel

binding pattern and thus significantly blocking the interaction between PD-1 and PD-L1 [35], but few C₂-symmetric small molecule immune checkpoint inhibitors have been reported.

In this study, we found that the linker seemed not necessary for the blocking efficiency of PD-1/PD-L1 interaction. The “linker + aryl” motif can be replaced with a six-membered aromatic ring, and the resulted compounds maintained satisfactory activities. Moreover, we designed and synthesized a series of C₂ symmetric compounds based on our newly found inhibitors, and some of the compounds displayed promising inhibitory activity against the PD-1/PD-L1 interaction with IC₅₀ value at the single nanomolar range. The cell-based PD-1/PD-L1 blockade bioassays indicated that these C₂-symmetric molecules could significantly inhibit the PD-1/PD-L1 interaction at the cellular level and restore the immune function of T cells at the safety concentrations. The discovery of these phenyl-linked symmetric small molecules showed the potential of simplified-linker and C₂-symmetric strategy, providing a basis for the development of symmetric small molecule inhibitors of PD-1/PD-L1 interaction.

2. Results and discussion

2.1. Design strategy

Through the summary of several previous research [29–31,35], we found that most triaryl scaffold small molecules with good PD-L1 binding ability shared common pharmacophore characteristics. The aryl region contributed significantly to the binding of inhibitors through hydrophobic interactions, such as π - π , π -alkyl and π - σ interactions (Fig. 2A). As the bridge between the biaryl core and the aryl ring, the linker did not show the key interaction with PD-L1 in some crystal structures (Fig. 2A) [32–35]. However, the effect of different linkers on the activity of inhibitors is significant, which gave rise to our interest in this part. Therefore, a classic triaryl scaffold molecule (A1) from Incyte Corporation [28] was employed as a lead compound, and the exploration of the “linker + aryl” motif was carried out in this research (Fig. 2B). Considering the advantages of C₂-Symmetric strategy in enhancing the ability of small molecules to inhibit the PD-1/PD-L1 interaction, it was applied in the optimization and the activity influenced by tail was investigated.

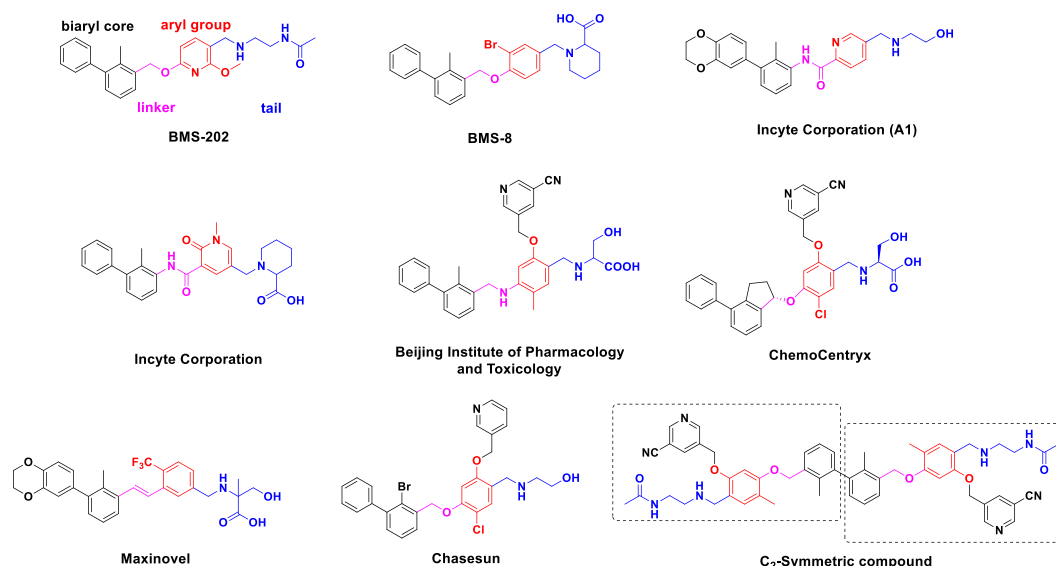
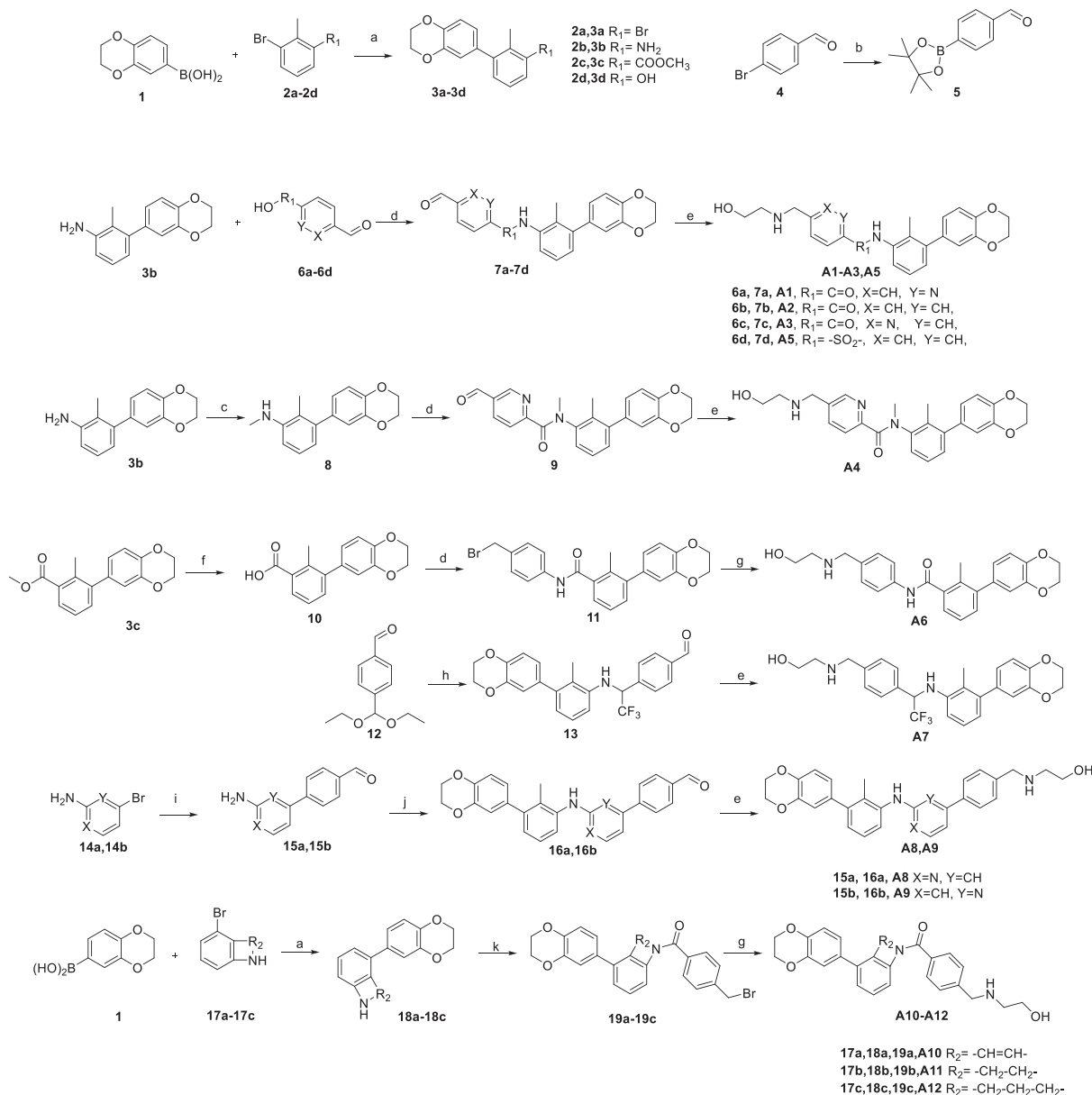


Fig. 1. Representative small molecule inhibitors targeting PD-L1.

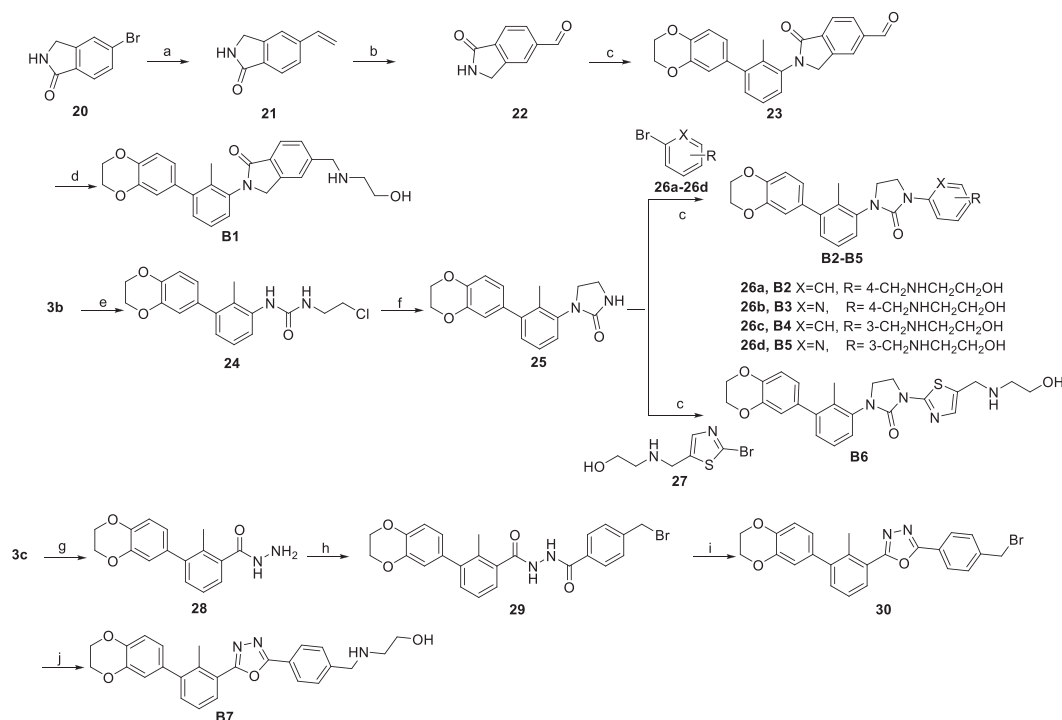


Scheme 1. Reagents and conditions: (a) XPhos-Pd G2, K_3PO_4 , THF; (b) Pd(dppf) Cl_2 , KOAc, Bis(pinacolato)diboron, 1,4-dioxane; (c) NaH, CH_3I , DMF; (d) DIPEA, HBTU, corresponding acid fragments, DCM; (e) NaBH_3CN , HAc, 2-aminoethanol, DCM; (f) LiOH, THF/ H_2O ; (g) Et_3N , 2-aminoethanol, DCM; (h) i) intermediate **3b**, EtOH; ii) TMSCF_3 , TBAT, THF; iii) HCl, MeOH; (i) $\text{Pd}(\text{PPh}_3)_4$, K_2CO_3 , intermediate **5**, THF/ H_2O ; (j) $\text{Pd}(\text{PPh}_3)_4$, X-Phos, Cs_2CO_3 , intermediate **3a**, 1,4-dioxane; (k) (n-Bu) $_4\text{NHSO}_4$, NaOH, 4-bromomethylbenzoyl chloride, DCM.

We designed compounds **A2-A12** to explore the linker's role in the interaction with PD-L1. The synthesis of compounds **A1-A12** is shown in **Scheme 1**. Carboxyl and sulfonic acid substituted aromatic hydrocarbons **6a-6d**, and intermediate **3b** was condensed and then obtained **A1-A3** and **A5** via a reductive amination reaction. Compound **A4** was obtained from the intermediate **3b** by amino methylation, condensation, and reductive amination reaction. The intermediate **3c** was hydrolyzed to obtain **10** and condensed with 4-aminobenzyl alcohol to obtain **11**. The intermediate **11** was formed into benzyl bromide, and then nucleophilic substitution was carried out to obtain **A6**. 4-(diethoxymethyl)benzaldehyde (**12**) and intermediate **3b** were dehydrated to obtain enamine, which reacted with TMSCF_3 , and then via de-protection and reductive amination reaction to obtain **A7**. Bromine and amino-substituted pyridine (**14a, 14b**) were coupled with intermediate **5** to obtain **15a** and **15b** and then reacted with intermediates **3a** to yield **16a**

and **16b** by the classical Suzuki-Miyaura coupling reaction. Through the $\text{Na}(\text{CN})\text{BH}_3$ -mediated reductive amination reaction, **16a**, and **16b** were converted to the desired compounds **A8-A9**. Intermediate **17a-17c** reacted with (1,4-benzodioxan-6-yl)boronic acid (**1**) to yield **18a-18c** by coupling reaction and reacted with acyl chloride to obtain the intermediate **19a-19c**, and finally, nucleophilic substitution was carried out to obtain **A10-A12**.

B1-B12 was designed for further optimization to validate linker and aryl group interact with PD-L1 as a whole motif, while **B13-B16** was designed to explore the influence of conformational constraints on tails. The synthesis route of compounds **B1-B7** is shown in **Scheme 2**. The intermediate **21** was obtained by coupling reaction, which was oxidized to **22**. Then the intermediate **23** was obtained by C-N coupling with the intermediate **3a**. In the last step, the desired compounds **B1** were prepared from **23** under $\text{Na}(\text{CN})\text{BH}_3$ -mediated reductive amination conditions as described above.



Scheme 2. Reagents and conditions: (a) Pd(PPh₃)₄, Tributyl (vinyl)tin, PhMe; (b) CuI, K₂CO₃, DMCHDA, PhMe; (c) RuCl₃, PhI(OAc)₂, corresponding bromo-aromatics, DCM; (d) NaBH₃CN, HAc, 2-aminoethanol, DCM; (e) 2-chloroethyl isocyanate, DCM; (f) NaH, DMF; (g) hydrazine hydrate, EtOH, refluxed; (h) (n-Bu)₄NHSO₄, NaOH, 4-bromomethylbenzoyl chloride, DCM; (i) POCl₃, refluxed; (j) Et₃N, 2-aminoethanol, DCM.

Intermediate **3b** reacted with 2-chloroethyl isocyanate to yield intermediate **24**, and cyclization gave intermediate **25**. The same C–N coupling is carried out with brominated aromatic hydrocarbons **26a–26d** and **27** to yield **B2–B6**, respectively. Intermediate **3c** reacted with hydrazine hydrate to obtain intermediate **28**, which is then condensed with 4-bromomethylbenzoyl chloride to yield **29**. Intermediate **29** was dehydrated and cyclized to intermediate **30** under the condition of phosphorus trichloride, and finally **B7** was obtained through nucleophilic substitution. The synthetic route of compounds **B8–B16** is outlined in Scheme 3. The intermediate **3d** reacted with bis(pinacolato)diboron to form intermediate **31**. **B8–B12** was obtained by coupling **31** with different substituted aromatic hydrocarbons (**32a–32c**, **33a–33c**) and then reductive amination. The intermediates **35** obtained by Suzuki coupling reacted with different substituted aminoalkanes to obtain **B13** and **B14** by further cyclization. The intermediate **39** was obtained by reductive amination with N-Boc protected glycine, further cyclization after de-protection yielding desired **B15**. **B16** was obtained by Suzuki coupling and nucleophilic substitution of bromo-substituted benzoazepine (**41**).

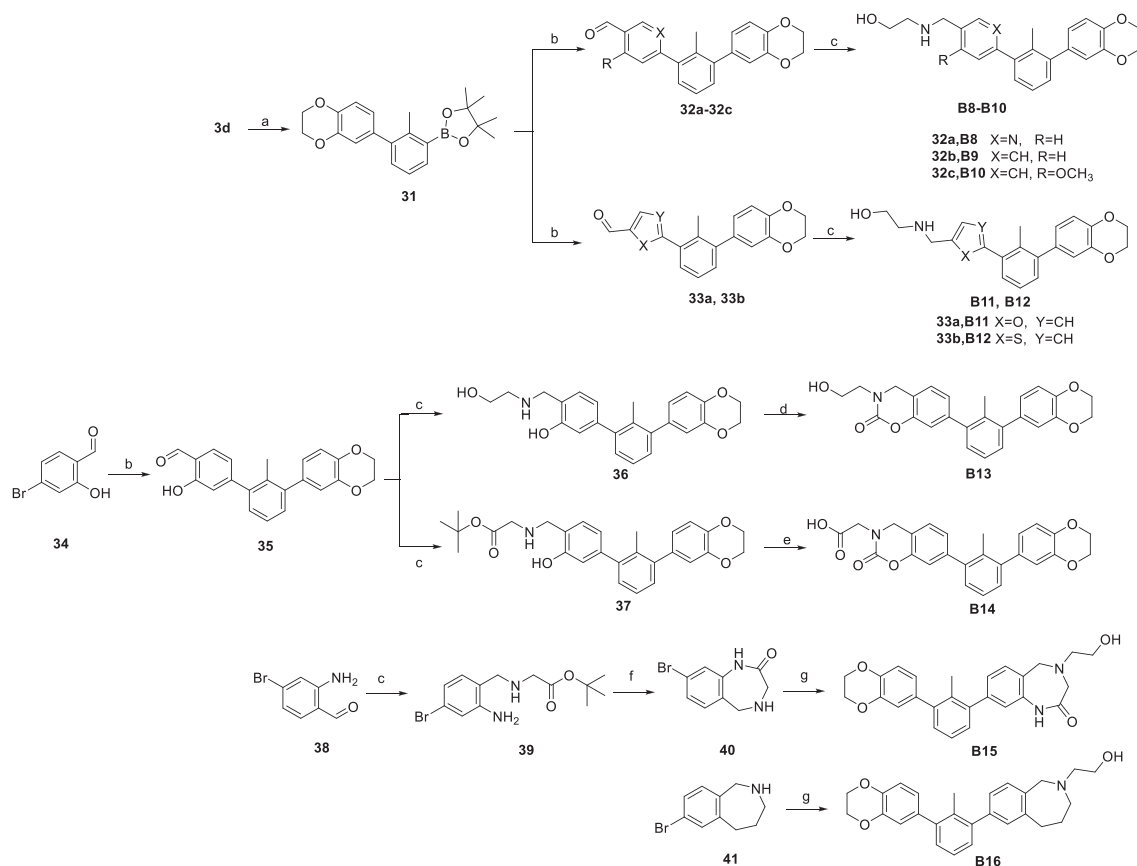
Through the introduction of C₂-symmetric strategy and exploration of the tail group, **C1–C15** was synthesized following the route in Scheme 4. The intermediates **17a** mentioned above were prepared into boronic acid pinacol ester intermediates **42**, which were then coupled with bromo-substituted indole to obtain biphenyl intermediates **43**, and **C1** was yield by condensation and substitution reaction. The desired compound **C2** is reduced from **C1**. Biphenol intermediate **46** was obtained from intermediate **2d** by a process similar to that of biphenyl **43** and prepared into boronic acid pinacol ester, and then reacted with different aryl aldehydes to yield **48a–48c** by the classical Suzuki–Miyaura coupling reaction. The desired compounds **C3–C5** were prepared from **48a–48c** under Na(CN)BH₃-mediated reductive amination conditions as described

above. The tail chain is modified by the intermediate **48c** reacting with different amino alcohols and amino acids to obtain **C6–C15**.

2.3. In vitro activity based on HTRF and discussion of SAR

At first, we evaluated different linkers, including a series of amide bond bioisosteres (Table 1). HTRF experiments showed that compounds (**A5**, **A7–A9**) substituted by bioisosteres did not retain the inhibitory activity of the amide bond linker (**A1**, in Incyte Corporation WO2017106634 [28]). Therefore, we speculated that the binding effect brought only by the amide bond was probably due to the special conformation caused by its special electron cloud distribution. Next, we retained the amide bond. When the aryl ring connected to it was changed from pyridine to benzene (**A2**), the binding efficacy was reduced by more than 400-folds. More interestingly, the amide bond inversion, methylation, and transposition of the pyridine N atom (**A3**, **A4**, and **A6**) significantly affect the blockade efficacy on PD-1/PD-L1 interaction of compound **A1**. From this, we assumed that the hydrogen bond interaction between amide linker and pyridine caused the aromatic region to be in a special dihedral conformation, thus increasing the interaction with PD-L1. Through the exploration of the biphenyl region (**A10–A12**), we found that the rigid conformation of the linker to the biphenyl region maybe not necessary, which further proves that the conformational restriction caused by the hydrogen bond between the amide bond and pyridine is an important factor affecting the binding efficacy of the compound to PD-L1.

Based on the above investigation, the structure–activity relationship was further explored by taking the “Linker + Aryl” as one motif (Table 2). Due to the important role of the aromatic ring in binding with PD-L1, we maintained the original aryl ring during further modification. Among the synthesized compounds, the rigid linker with conformational restriction (**B1–B7**) did not show



Scheme 3. Reagents and conditions: (a) i) TiF_2O , Pyridine, DCM; ii) Bis(pinacolato)diboron, Pd (dppf) Cl_2 , KOAc, 1,4-dioxane; (b) Pd (dppf) Cl_2 -DCM, KOAc, corresponding bromoaromatics, 1,4-dioxane; (c) NaBH_3CN , HAc, corresponding amines, DCM; (d) i) Triphosgene, Et_3N , DCM; ii) HCl, MeOH; (e) i) TBSOTf, Pyridine, DCM; ii) Triphosgene, Et_3N , DCM; iii) CF_3COOH , DCM; (f) i) CF_3COOH , DCM; ii) PhMe, refluxed; (g) i) Pd (dppf) Cl_2 -DCM, KOAc, 1,4-dioxane; ii) Et_3N , 2-bromoethanol, DCM.

satisfactory activity. However, the IC_{50} values of compounds **B8** and **B9** were 19.6 nM and 16.2 nM, and the inhibitory rates of compounds **B10** were 94.0% at 1 μM . These results indicated that linker and aryl ring indeed interact with PD-L1 protein as a whole, and the six-membered aromatic ring can be used as a complete motif to maintain good inhibitory activity, while the compound (**B11** and **B12**) containing five-membered aromatic ring didn't show promising blockade efficacy. It should be noted that the poor activity of **B1–B7** suggested that the rigid linker may affect the interaction with PD-L1 largely by limiting the conformation of small molecule blockers.

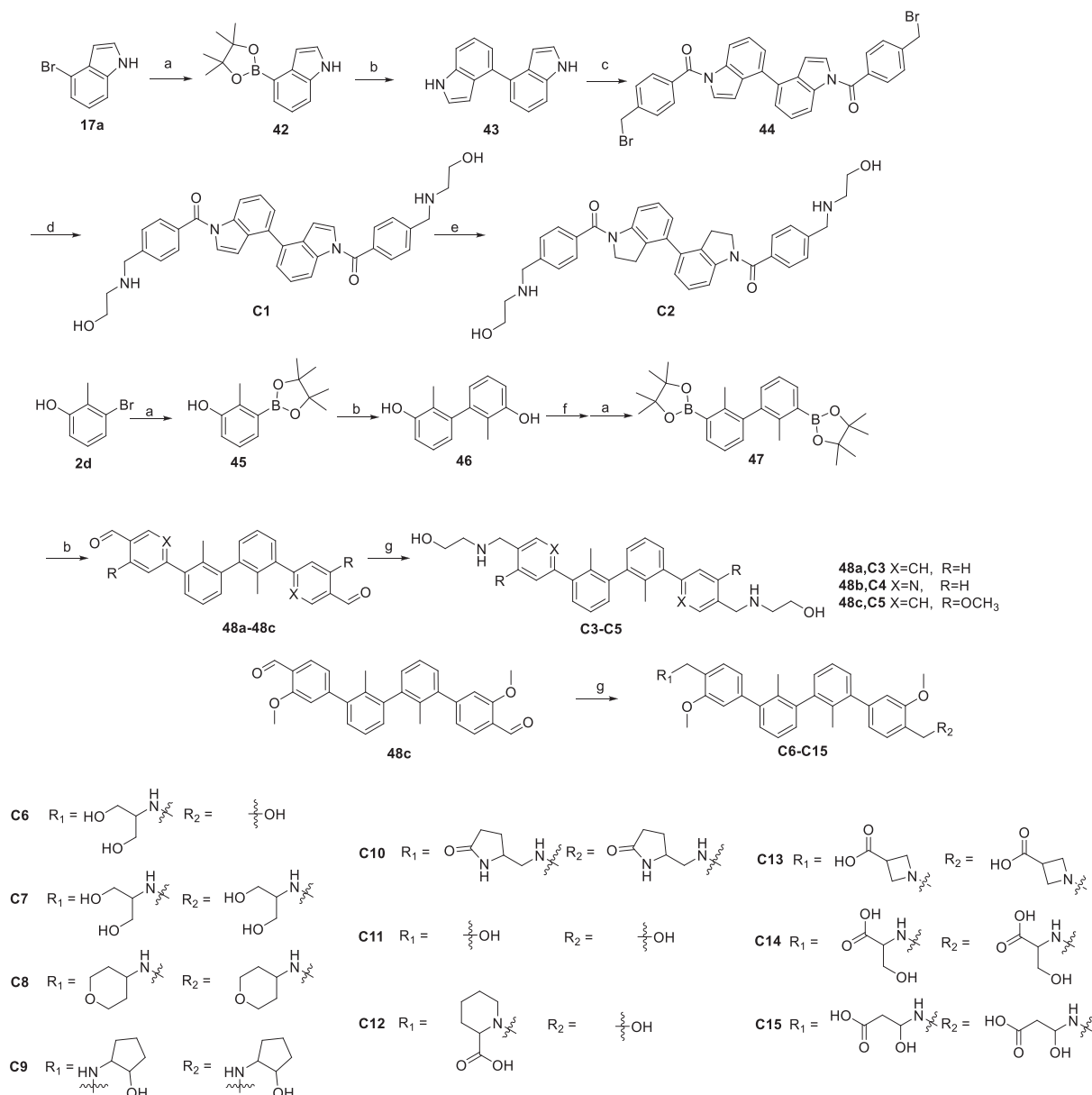
The tail exposed to the solvent region has a key hydrogen bond interaction with PD-L1, so we also explored the conformational restriction in this part (Table 2). However, compounds **B13–B16** showed no effective inhibitory activity, which indicated that flexible side chain was crucial for the maintenance of compound activity.

Next, we designed and synthesized a series of C_2 -symmetric PD-L1 inhibitors (Table 3 and 4). **C1** and **C2** did improve their activity compared with their monomers **A10** and **A11**, but interestingly, **C3** and **C4** were not optimized by the dimerization strategy (**C3** vs. **B9**, **C4** vs. **B8**). Considering that symmetric compounds will inevitably introduce more hydrophobic aromatic rings and the tail chain has a great influence on the activity, the influence of different tail chains on the activity should be further explored, leading to the further optimization of **C5** (Table 4). HTRF results showed that the tail chain containing alcohol hydroxyl and secondary amines group could maintain the inhibitor activity, such as **C6** (IC_{50} = 48.7 nM), **C8**

(IC_{50} = 34.4 nM), **C9** (IC_{50} = 36.4 nM). However, the activity of **C10**, **C11** and **C12** containing only secondary amine and hydroxyl in the tail decreased significantly, indicating that both N and O atoms play important roles as hydrogen bond donors or acceptors in interaction with PD-L1. In view of the excellent inhibitory activity of **C13** with carboxyl group tails, we introduced natural amino acids into the tail to obtain **C14** and **C15** with satisfactory IC_{50} of 3.90 nM and 4.01 nM, respectively which may be caused by more complex hydrogen bond donors and receptors. All in all, it suggested that the hydrophilicity and hydrogen-bond web of the tail extending to the solvent region is crucial for inhibitor activity.

2.4. Low non-specific cytotoxicity of **C13–C15**

As inhibitors of the PD-1/PD-L1 interaction, we expect these compounds to act by blocking immune checkpoints rather than by direct cytotoxicity. In addition, the non-specific cytotoxicity of these compounds may affect their evaluation at the cellular level. Therefore, the toxicity of compounds showing promising activity on the biochemical level was evaluated using CCK-8 assays. Human PBMCs were treated with compounds at a gradient concentration for 48 h, and none of the compounds showed significant cytotoxicity at the concentration of 3 μM (Fig. 3). More importantly, **C13–C15** did not show cytotoxicity at concentrations as high as 10 μM in human pancreatic ductal epithelial cells (HPDE6-C7) and human hepatocytes (HL7702).



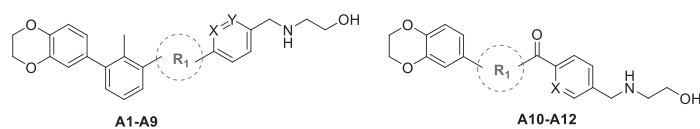
Scheme 4. Reagents and conditions: (a) Bis(pinacolato)diboron, Pd (dppf)Cl₂, KOAc, 1,4-dioxane; (b) Pd (dppf)Cl₂-DCM, KOAc, corresponding bromo-aromatics, 1,4-dioxane; (c) (n-Bu)₄NHSO₄, NaOH, 4-bromomethylbenzoyl chloride, DCM; (d) Et₃N, 2-aminoethanol, DCM; (e) NaBH₃CN, HAc; (f) Tf₂O, Pyridine, DCM; (g) NaBH₃CN, HAc, corresponding amines, DCM.

2.5. Demonstration of immune checkpoint inhibition of C13–C15 in cell-based PD-1/PD-L1 signaling assays

Above, we evaluated the ability of the compound to block the PD-1/PD-L1 interaction at the protein level, but the binding and blocking ability of the small molecule inhibitor at the cellular level is crucial to its inhibitory efficiency. Therefore, we selected the compounds with excellent performance in the HTRF experiment for cell-based PD-1/PD-L1 blockade assay. Jurkat T cells were modified to constitutively express PD-1 and carry luciferase reporter genes driven by the TCR-inducible NFAT response element. TCR-mediated luminescence was inhibited by PD-1/PD-L1 interaction during co-culture. However, when small molecule inhibitors were added to the co-cultured cell model, the blocking of the PD-1/PD-L1 interaction would lead to an increase in the luminescence intensity, which is the indicator of the blocking ability of PD-1/PD-L1 at the

cell level measured by NFAT assay [35]. In the NFAT reporter assay, the concentration of the compounds was less than 10 μM, which is within the range of the non-toxic concentration. To ensure the accuracy of cell-based PD-L1 blockade bioassay, PD-L1 antibody (Keytruda) was used as a positive control at a concentration (5 μg/mL) that could reach maximum luminescence value (RLU_{max}). Fig. 4 shows that **C13–C15** dose-dependently released PD-L1-mediated inhibition of PD-1-expressing Jurkat T cells with EC₅₀ values of 0.104 μM, 0.775 μM, and 0.376 μM, respectively (Table 5). The RLU_{max} of **C13** is 35761 (Table 5), which is equivalent to that of the PD-L1 antibody. The good dose-dependence and promising EC₅₀ indicated that compound **C13–C15** could inhibit the PD-1/PD-L1 interaction at the cellular level.

Table 1
Activities of compounds **A1–A12** in inhibition of the PD-1/PD-L1 interaction.



Compound	R ₁	X	Y	IC ₅₀ (nM) ^a
A1 (in Incyte Corporation WO2017106634)		N	C	5.04
A2		C	C	>1000
A3		C	N	>1000
A4		N	C	764
A5		C	C	>1000
A6		C	C	>1000
A7		C	C	>1000
A8		C	C	>1000
A9		C	C	>1000
A10		C	–	>1000
A11		C	–	150
A12		C	–	>1000

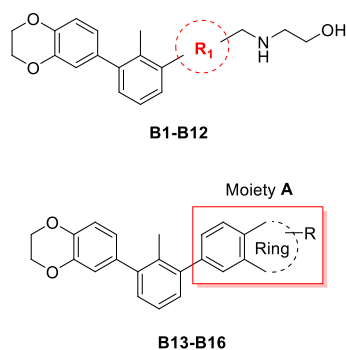
^a The data are generated from two independent experiments.

2.6. Effect of C13–C15 on IFN- γ production

In the tumor microenvironment, the binding of PD-L1 to PD-1 leads to tyrosine phosphorylation in the intracellular domain of immune cells and recruitment of tyrosine phosphatase SHP-2 [36], thereby reducing downstream activation signals of the TCR pathway and the generation of some cytokines [37]. Blockade of the PD-1/PD-L1 interaction could reactivate T cell function, such as the secretion of IFN- γ , which suggested the inhibition of tumor immune escape through the PD-L1 pathway [38]. Considering HTRF

and cell-based PD-L1 blockade activity, **C13–C15** were further assessed for ability to restore the immunity repressed by the PD-1/PD-L1 pathway activation. The results showed that all three compounds increased IFN- γ release in a dose-dependent manner. As expected, the compound's activity to restore T-cell IFN- γ secretion was consistent with cell-based PD-L1 blockade bioassay. As shown in Fig. 5, compound **C15** increased the amount of IFN- γ 5-fold against the control group at 3 μ M, which was comparable to the effect of monoclonal antibody. Compound **C14** was the least effective but still showed a nearly 4-fold increase in IFN- γ release at

Table 2
Activities of compounds **B1–B16** in inhibition of the PD-1/PD-L1 interaction.



Compound	R ₁ or Moiety A	Inhibition rate ^a	IC ₅₀ (nM) ^{a,b}
B1		—	>1000
B2		—	>1000
B3		—	>1000
B4		—	>1000
B5		—	>1000
B6		—	>1000
B7		—	>1000
B8		—	19.6
B9		—	16.2
B10		94.0% (at 1 μM)	N.T.
B11		—	191
B12		65.4% (at 1 μM)	N.T.
B13		25.2% (at 5 μM)	N.T.

(continued on next page)

Table 2 (continued)

Compound	R ₁ or Moiety A	Inhibition rate ^a	IC ₅₀ (nM) ^{a,b}
B14		0.54% (at 5 μM)	N.T.
B15		12.5% (at 5 μM)	N.T.
B16		2.76% (at 5 μM)	N.T.
A1	—	—	5.04

^a The data are generated from two independent experiments.

^b N.T., not tested.

3 μM. **C13** and **C15** showed significant IFN-γ induction at non-cytotoxic concentrations, suggesting its potential to be further developed as a PD-L1 inhibitor to improve tumor immune microenvironment.

2.7. hERG blockade evaluation of compounds

Given the multiple diphenyl groups in compounds that may cause inhibition of the hERG potassium channel and the attractive potential of compounds **C13–C15** for further development as small-molecule PD-L1 inhibitors, we evaluated their hERG channel blocking effects. As expected, compound **C13–C15** did not show the same alarming cardiotoxicity as compound **B9** (Table 6), suggesting that these compounds may indeed be further explored as novel small-molecule PD-L1 inhibitors.

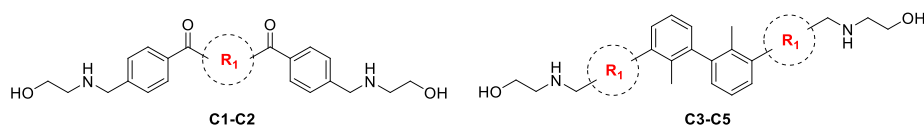
2.8. Docking analysis of C13 and C15 with the dimeric PD-L1

To explore the possible binding mode of compound **C13** and **C15** with dimeric PD-L1, computational docking and molecular dynamics (MD) were performed. First, the complex of dimeric PD-L1 protein (PDB code: 6RPG) [35] with **C13** or **C15** was simulated for 100ns. As shown in Fig. S1, the root-mean-square deviation (RMSD) became stable at around 1.5 Å, indicating that dynamic equilibrium was attained. As expected, the biphenyl cores of compounds **C13** and **C15** occupied hydrophobic chambers composed of hydrophobic amino acids such as Met115 and Ala121. The interaction of phenyl-linker with Tyr56 contributes to the binding of the compounds to dimeric PD-L1 (Fig. 6A, 6B). The tail containing many hydrogen bond donors and receptors interacts with Gln66, Lys124, and Asp122 through a complex hydrogen bond network. Interestingly, we found that **C15** with a relatively flexible tail seems to interact with Lys124 much more significantly than **C13**, suggesting that a flexible tail may be a superior strategy (Fig. 6C). All in all, the docking results proved that the linker and aryl group could interact with the protein as a whole, and the flexible tail with multiple hydrogen bond donors and receptors could not only provide better physicochemical properties but also contribute to the binding efficacy of the compounds.

3. Conclusion

To summarize, the discovery of these phenyl-linked symmetric small molecules showed the potential of simplified-linker and C₂-symmetric strategy and provided a basis for developing symmetric

Table 3
Activities of compounds **C1–C5** in inhibition of the PD-1/PD-L1 interaction.



Compound	R1	IC ₅₀ (nM) ^a
C1		309
C2		18.6
C3		45.6
C4		>1000
C5		48.6

^a The data are generated from two independent experiments.

small molecule inhibitors of PD-1/PD-L1 interaction. Moreover, computational docking and dynamic simulation demonstrated that both **C13** and **C15** displayed strong binding to PD-L1 dimeric. Given the potential for the development of them as small molecule inhibitors of PD-1/PD-L1 interaction, further optimization is taking place in our lab.

4. Experimental procedures

4.1. Chemistry

¹H NMR and ¹³C NMR spectra were recorded at 500 MHz using a Bruker AVANCE III spectrometer in CDCl₃, or DMSO-*d*₆ solution, with tetramethylsilane (TMS) serving as internal standard. Chemical shift values (δ) were reported in ppm. Multiplicities are recorded by the following abbreviations: s, singlet; d, double; t, triplet; q, quartet; m, multiplet; J, coupling constants (Hz). High-resolution mass spectrum (HRMS) was obtained from Agilent Technologies 6224 TOF LC/MS. The purities of compounds for biological testing were assessed by NMR and HPLC, and the purities were ≥95%. The analytical HPLC was performed on an Agilent 1260 Infinity II (LC03) machine and a C18 reversed-phase column (Agilent Eclipse XDB-C18, 4.6*250 mm, 5 μm), with a flow rate of 1.0 mL/min, the detection by UV absorbance at a wavelength of 254 nm, the column temperature was 25 °C, eluting with water (0.1% trifluoroacetic acid) as A phase and methanol as B phase (0 min, A phase: 90%, B phase: 10%; 10 min, A phase: 10%, B phase: 90%; 15 min, A phase: 10%, B phase: 90%; 20 min, A phase: 90%, B phase: 10%; 30 min, A phase: 90%, B phase: 10%). Unless otherwise noted, reagents and solvents were obtained from commercial suppliers and without further purification.

General procedure A: (for the synthesis of compounds **3b–3d**, **18a–18c**) (1,4-Benzodioxan-6-yl)boronic acid (11.112 mmol), bromobenzene (9.6 mmol), Pd-Xphos (224 mg, 0.28 mmol) was added

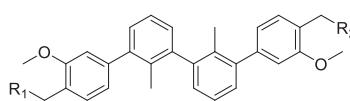
to 0.5 N potassium phosphate solution and tetrahydrofuran in the flask. The mixture was heated to reflux overnight under a nitrogen atmosphere. After TLC monitoring, the mixture was concentrated under vacuum. The residue was diluted with water (100 mL) and extracted with ethyl acetate (100 mL × 3), washed by saturated brine (50 mL × 2) and dried over anhydrous sodium sulfate. The crude product was purified by column chromatography to afford the product.

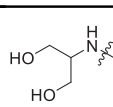
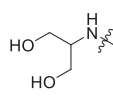
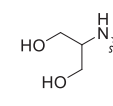
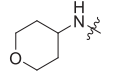
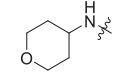
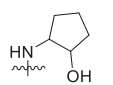
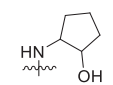
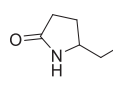
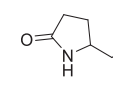
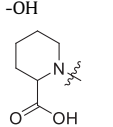
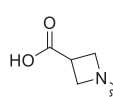
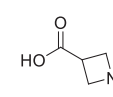
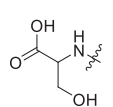
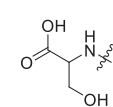
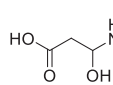
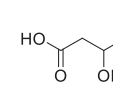
General procedure B: (for the synthesis of compounds **5**, **31**, **42** and **45**) [1,1'-bis (diphenylphosphine) ferrocene] palladium dichloride (200 mg, 0.27 mmol), and potassium acetate (1.589 g, 16.2 mmol) was added into 30 mL 1,4-dioxane solution of bromobenzene (5.4 mmol) and Bis(pinacolato)diboron (1.647 g, 6.49 mmol). The mixture was heated to reflux overnight under a nitrogen atmosphere. After extraction and concentrated, the residue was purified by column chromatography to afford the product.

General procedure C: (for the synthesis of compounds **7a–7d**, **9** and **11**) Carboxylic acids (0.66 mmol), DIPEA (161 mg, 1.254 mmol) and DCM 10 mL were added in the flask and stirred at room temperature for 10 min. HBTU (500 mg, 1.32 mmol) was added, and the mixture was stirred at room temperature for another 10 min, and amines (0.66 mmol) was added. After it was fully reacted, the mixture was concentrated under vacuum. The residue was diluted with water (25 mL) and extracted with ethyl acetate (25 mL × 3), washed by saturated brine (25 mL × 2) and dried over anhydrous sodium sulfate. The crude product was purified by column chromatography to afford the product.

General procedure D: (for the synthesis of compounds **A1–A5**, **A7–A9**, **B1**, **B7–B12**, **36**, **37**, **39** and **C3–C15**) To a flask was added benzaldehydes (0.119 mmol), amines (0.659 mmol) and DMF (6 mL). The reaction was stirred for 1 h at room temperature. Then sodium cyanoborohydride (41 mg, 0.659 mmol) and acetic acid (41 μL, 0.6 mmol) were added and the reaction was stirred at room temperature overnight. After it was fully reacted, the mixture was

Table 4
Activities of compounds **C6–C15** in inhibition of the PD-1/PD-L1 interaction.



Compound	R1	R2	IC50 (nM) ^a
C6		-OH	48.7
C7			>1000
C8			34.4
C9			36.4
C10			139
C11	-OH	-OH	481
C12		-OH	472
C13			4.23
C14			3.90
C15			4.01
A1	—	—	5.04

^a The data are generated from two independent experiments.

diluted with water (50 mL) and extracted with ethyl acetate (50 mL × 3), washed by saturated brine (25 mL × 2) and dried over

anhydrous sodium sulfate. After solvent removal, the crude product was purified by column chromatography to afford the product.

General procedure E: (for the synthesis of compounds **A6**, **A10–A12** and **C1**) Benzyl bromides (0.11 mmol), aminoethanol (21 mg, 0.33 mmol) and DCM (10 mL) were added into the flask, then Et₃N (35 mg, 0.33 mmol) was added and stirred at room temperature. After solvent removal, the residue was purified by column chromatography to afford the product.

General procedure F: (for the synthesis of compounds **19a–19c**, **29** and **44**) Amines (4.35 mmol), (n-Bu)₄NHSO₄ (27 mg, 0.08 mmol) and NaOH (39.8 mg, 1 mmol) were dissolved in DCM (11 mL). DCM solution of chlorides (139 mg, 0.597 mmol) was then added to the above solution and stirred at room temperature. After TLC monitoring and solvent removal, the residue was purified by column chromatography to give the product.

General procedure G: (for the synthesis of compounds **23** and **B2–B6**) To a solution of amines (0.39 mmol), RuCl₃ (0.8 mg, 0.00039 mmol), Ph(OAc)₂ (42 mg, 0.13 mmol) in DCM (5 mL) was added bromo-aromatics (0.5 mmol) and stirred at room temperature. After TLC monitoring, the mixture was concentrated under vacuum. The residue was diluted with water (10 mL) and extracted with ethyl acetate (10 mL × 3), washed by saturated brine (5 mL × 2) and dried over anhydrous sodium sulfate. The crude product was purified by column chromatography to afford the product.

General procedure H: (for the synthesis of compounds **32a–32c**, **33a–33c**, **35**, **43**, **46** and **48a–48c**) A solution of borate diesters (0.645 mmol), bromo-aromatics (100 mg, 0.537 mmol) in 1,4-dioxane (5 mL) was added Pd(dppf)Cl₂·DCM (22 mg, 0.027 mmol) and KOAc (158 mg, 1.6 mmol). The atmosphere of the reaction system was replaced by nitrogen three times and refluxed. After the reaction was completed, the residue was diluted with water (20 mL) and extracted with ethyl acetate (20 mL × 3), washed by saturated brine (10 mL × 2) and dried over anhydrous sodium sulfate. The crude product was purified by column chromatography to afford the product.

4.1.1. 6-(3-bromo-2-methylphenyl)-2,3-dihydrobenzo[b][1,4]dioxine **3a**

(1,4-Benzodioxan-6-yl)boronic acid (**1**, 2 g, 11.112 mmol), 1,3-dibromo-2-methylbenzene (**2a**, 2.777 g, 11.112 mmol), Pd(dppf)Cl₂ (204 mg, 0.28 mmol), KOAc (3.234 g, 33 mmol), and 50 mL tetrahydrofuran were added into flask. The mixture was heated to reflux overnight under a nitrogen atmosphere. After TLC monitoring, 4 g colorless oily liquid was obtained by column chromatography. Yield: 80%; ¹H NMR (500 MHz, Chloroform-*d*) δ 7.55–7.51 (m, 1H), 7.17–7.13 (m, 1H), 7.05 (t, *J* = 7.8 Hz, 1H), 6.90 (d, *J* = 8.2 Hz, 1H), 6.80 (d, *J* = 2.0 Hz, 1H), 6.74 (dd, *J* = 8.2, 2.1 Hz, 1H), 4.30 (s, 4H), 2.34 (s, 3H). ESI-MS: *m/z* = 307 [M+H]⁺.

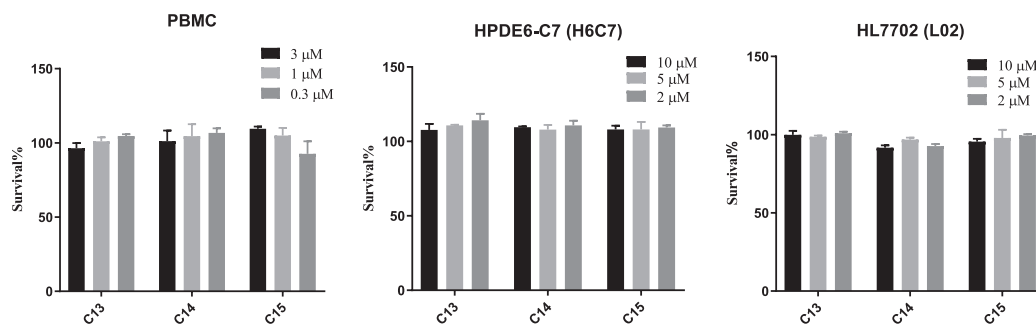


Fig. 3. Cytotoxicity of compound **C13–C15** on HPDE6-C7, HL7702, and PBMC. Data are shown as mean ± SD.

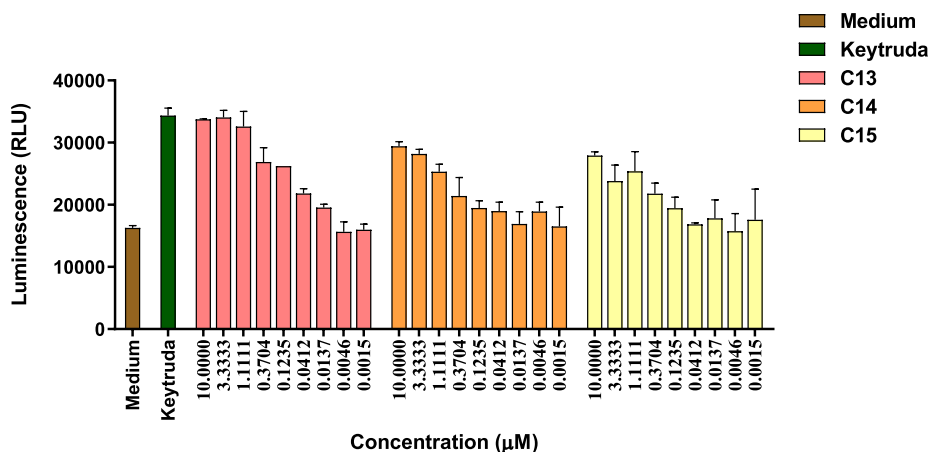


Fig. 4. Cell-based PD-1/PD-L1 interaction blockade activity (luminescence intensity) of Keytruda, **C13**, **C14**, and **C15**. PD-1/PD-L1 immune checkpoint bioassay performed in duplicates by co-culturing PD-L1/OS8-expressing Hep3B cells and NFAT/PD-1-expressing Jurkat cells for 6 h in the presence of varying concentrations of the small molecules and 5 µg/mL Keytruda.

Table 5
Cell-based blockade activity of PD-1/PD-L1 interaction.

Compounds	EC ₅₀ (nM) ^a	RLU _{max}
C13	104	35761
C14	775	30595
C15	376	27050

^a The data are generated from two independent experiments.

Table 6
hERG blockade rate of compound **B9**, **B10**, **C13**, **C14** and **C15**.

Compound	hERG blockade rate at 10 µM
B9	97.95%
B10	4.71%
C13	3.93%
C14	-0.67%
C15	7.72%

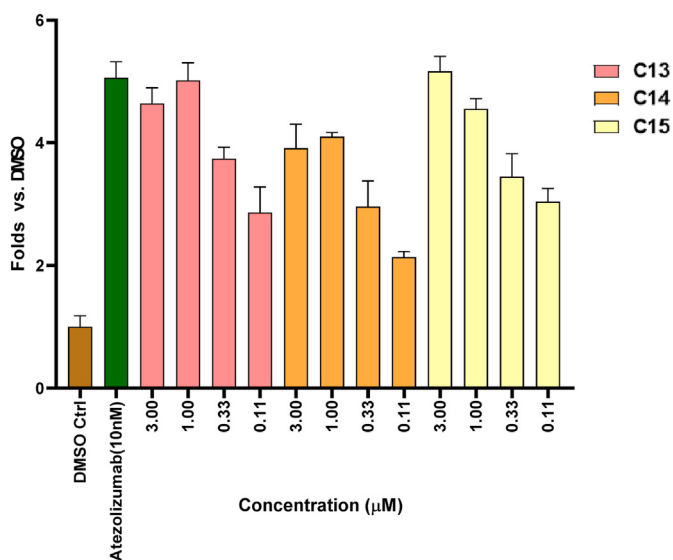


Fig. 5. The activity of **C13**, **C14**, **C15**, and Atezolizumab on IFN-γ production. Each group was compared with the DMSO group to get a fold. Data are shown as mean ± SD.

4.1.2. 3-(2,3-dihydrobenzo[b][1,4]dioxin-6-yl)-2-methylaniline **3b**

General procedure A. Yield: 99%; ¹H NMR (500 MHz, Chloroform-*d*) δ 7.05 (t, *J* = 7.7 Hz, 1H), 6.90 (d, *J* = 8.2 Hz, 1H), 6.83 (d, *J* = 2.0 Hz, 1H), 6.78 (dd, *J* = 8.2, 2.1 Hz, 1H), 6.70 (d, *J* = 7.7 Hz, 2H), 4.30 (s, 4H), 2.09 (s, 3H). ESI-MS: *m/z* = 242 [M+H]⁺.

4.1.3. methyl 3-(2,3-dihydrobenzo[b][1,4]dioxin-6-yl)-2-methylbenzoate **3c**

General procedure A. Yield: 95%; ¹H NMR (500 MHz, Chloroform-*d*) δ 7.77 (dd, *J* = 7.7, 1.6 Hz, 1H), 7.34 (dd, *J* = 7.5, 1.5 Hz, 1H), 7.24 (d, *J* = 7.6 Hz, 1H), 6.90 (d, *J* = 8.2 Hz, 1H), 6.80 (d, *J* = 2.1 Hz, 1H), 6.74 (dd, *J* = 8.2, 2.1 Hz, 1H), 4.30 (s, 4H), 3.91 (s, 3H), 2.43 (s, 3H). ¹³C NMR (126 MHz, CDCl₃) δ 168.87, 143.15, 143.06, 142.75, 136.74, 134.86, 133.29, 131.32, 128.95, 125.15, 122.52, 118.20, 116.91, 77.28, 77.23, 77.02, 76.77, 64.43, 64.41, 52.01, 18.49, 18.44. ESI-MS: *m/z* = 285 [M+H]⁺.

4.1.4. 3-(2,3-dihydrobenzo[b][1,4]dioxin-6-yl)-2-methylphenyl trifluoromethanesulfonate **3d**

General procedure A. Yield: 89%; ¹H NMR (500 MHz, Chloroform-*d*) δ 7.28 (d, *J* = 7.7 Hz, 0H), 7.26 (s, 1H), 7.25–7.20 (m, 2H), 6.92 (d, *J* = 8.2 Hz, 1H), 6.81 (d, *J* = 2.0 Hz, 1H), 6.76 (dd, *J* = 8.2, 2.1 Hz, 1H), 4.31 (s, 4H), 2.27 (s, 3H). ESI-MS: *m/z* = 375 [M+H]⁺.

4.1.5. 4-(4,4,5,5-tetramethyl-1,3,2-dioxaborolan-2-yl)benzaldehyde **5**

General procedure B. Yield: 96%; ¹H NMR (500 MHz, Chloroform-*d*) δ 10.05 (s, 1H), 7.99–7.93 (m, 2H), 7.89–7.83 (m, 2H), 1.36 (s, 12H); ESI-MS: *m/z* = 233 [M+H]⁺.

4.1.6. *N*-(3-(2,3-dihydrobenzo[b][1,4]dioxin-6-yl)-2-methylphenyl)-5-formylpicolinamide **7a**

General procedure C. Yield: 64%; ESI-MS: *m/z* = 375 [M+H]⁺.

4.1.7. *N*-(3-(2,3-dihydrobenzo[b][1,4]dioxin-6-yl)-2-methylphenyl)-4-formylbenzamide **7b**

General procedure C. Yield: 70%; ESI-MS: *m/z* = 374 [M+H]⁺.

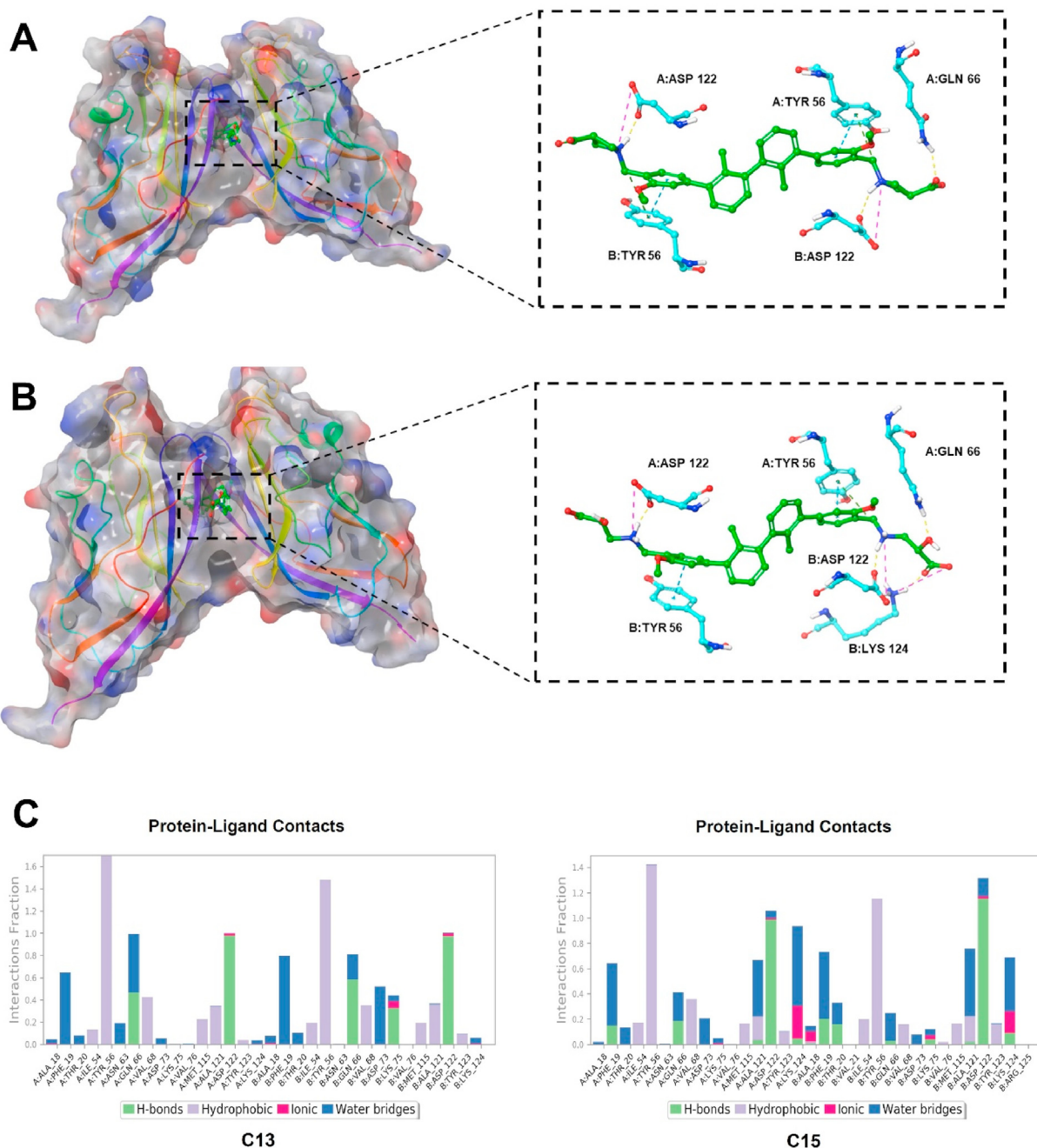


Fig. 6. MD simulations and Docking analysis of the interaction of compound **C13** and **C15** with dimeric PD-L1 protein (PDB code: 6RPG). (A) protein-ligand interaction between PD-L1 dimeric and compound **C13**; (B) protein-ligand interaction between PD-L1 dimeric and compound **C15**; (C) protein-ligand contacts between PD-L1 dimeric and compound **C13** and **C15**.

4.1.8. *N*-(3-(2,3-dihydrobenzo[*b*] [1,4]dioxin-6-yl)-2-methylphenyl)-6-formylnicotinamide **7c**

General procedure C. Yield: 64%; ESI-MS: $m/z = 375$ [M+H]⁺.

4.1.9. *N*-(3-(2,3-dihydrobenzo[*b*] [1,4]dioxin-6-yl)-2-methylphenyl)-4-formylbenzenesulfonamide **7d**

General procedure C. Yield: 60%; ESI-MS: $m/z = 410$ [M+H]⁺.

4.1.10. 3-(2,3-dihydrobenzo[*b*] [1,4]dioxin-6-yl)-*N*,2-dimethylaniline **8**

3b (100 mg, 0.4 mmol) and anhydrous DMF (10 mL) were added in the flask. NaH (10 mg, 0.4 mmol) was added at 0 °C under

nitrogen atmosphere. The mixture was raised to room temperature and stirred for 1 h. CH₃I (59 mg, 0.4 mmol) were added and stir at room temperature. After TLC monitoring, saturated NH₄Cl solution was added. The mixture was extracted with EA and NaHCO₃, and organic layer dried with anhydrous sodium sulfate, and concentrated to remove the solvent. 25 mg **8** was obtained, which was directly used for the next step without purification. Yield: 80%; ESI-MS: $m/z = 256$ [M+H]⁺.

4.1.11. *N*-(3-(2,3-dihydrobenzo[*b*] [1,4]dioxin-6-yl)-2-methylphenyl)-6-formyl-*N*-methylnicotinamide **9**

General procedure C. Yield: 65%; ESI-MS: $m/z = 389$ [M+H]⁺.

4.1.12. *N*-(3-(2,3-dihydrobenzo[*b*] [1,4]dioxin-6-yl)-2-methylphenyl)-5-(((2-hydroxyethyl)amino)methyl)picolinamide **A1**

General procedure D. Yield: 20%; HPLC: t_R 13.313 min, purity 95.63%. 1H NMR (500 MHz, Chloroform-*d*) δ 10.11 (s, 1H), 8.59 (d, $J = 2.1$ Hz, 1H), 8.28 (d, $J = 7.9$ Hz, 1H), 8.21 (d, $J = 8.1$ Hz, 1H), 7.89 (dd, $J = 8.1, 2.1$ Hz, 1H), 7.29 (t, $J = 7.9$ Hz, 1H), 7.07 (d, $J = 7.6$ Hz, 1H), 6.91 (d, $J = 8.2$ Hz, 1H), 6.87–6.73 (m, 2H), 4.31 (s, 4H), 3.94 (s, 2H). ^{13}C NMR (126 MHz, $CDCl_3$) δ 160.98, 148.08, 146.99, 142.01, 141.61, 141.40, 137.72, 136.19, 135.10, 134.20, 125.45, 125.25, 125.03, 121.54, 121.20, 119.67, 117.19, 115.84, 76.25, 76.20, 76.00, 75.75, 63.40, 60.07, 49.65, 49.62, 13.95. ESI-MS: $m/z = 420$ [M+H] $^+$. HRMS (ESI) for $C_{24}H_{25}N_3O_4$ [M+H] $^+$, calcd: 420.1923, found: 420.1931.

4.1.13. *N*-(3-(2,3-dihydrobenzo[*b*] [1,4]dioxin-6-yl)-2-methylphenyl)-4-(((2-hydroxyethyl)amino)methyl)benzamide **A2**

General procedure D. Yield: 25%; HPLC: t_R 12.454 min, purity 95.42%. 1H NMR (500 MHz, Chloroform-*d*) δ 7.88 (dd, $J = 8.3, 6.4$ Hz, 3H), 7.73 (s, 1H), 7.46 (d, $J = 8.2$ Hz, 2H), 7.28 (d, $J = 7.8$ Hz, 1H), 7.10 (dd, $J = 7.7, 1.4$ Hz, 1H), 6.91 (d, $J = 8.2$ Hz, 1H), 6.82 (d, $J = 2.1$ Hz, 1H), 6.77 (dd, $J = 8.2, 2.1$ Hz, 1H), 4.30 (s, 4H), 3.90 (s, 2H), 3.70–3.66 (m, 2H), 2.84–2.81 (m, 2H), 2.23 (s, 3H). ^{13}C NMR (126 MHz, DMSO) δ 165.71, 146.79, 143.43, 143.00, 142.35, 137.41, 134.89, 133.23, 131.94, 129.65, 127.96, 127.86, 126.63, 126.54, 126.39, 125.99, 122.49, 118.05, 117.31, 64.58, 64.55, 62.89, 60.23, 40.55, 40.46, 40.38, 40.29, 40.22, 40.13, 40.05, 39.96, 39.88, 39.79, 39.63, 39.46, 16.09. ESI-MS: $m/z = 419$ [M+H] $^+$. HRMS (ESI) for $C_{25}H_{26}N_2O_4$ [M+H] $^+$, calcd: 419.1971, found: 419.1990.

4.1.14. *N*-(3-(2,3-dihydrobenzo[*b*] [1,4]dioxin-6-yl)-2-methylphenyl)-6-(((2-hydroxyethyl)amino)methyl)nicotinamide **A3**

General procedure D. Yield: 20%; 1H NMR (500 MHz, Chloroform-*d*) δ 9.08 (s, 1H), 8.24 (d, $J = 7.8$ Hz, 1H), 7.42 (t, $J = 9.1$ Hz, 2H), 7.19 (d, $J = 7.9$ Hz, 1H), 7.10 (d, $J = 7.6$ Hz, 1H), 6.86 (d, $J = 8.2$ Hz, 1H), 6.81–6.68 (m, 2H), 4.26 (s, 4H), 4.15 (s, 2H), 3.75 (s, 2H), 2.16 (s, 3H). ESI-MS: $m/z = 420$ [M+H] $^+$. HRMS (ESI) for $C_{24}H_{25}N_3O_4$ [M+H] $^+$, calcd: 420.1923, found: 420.1914.

4.1.15. *N*-(3-(2,3-dihydrobenzo[*b*] [1,4]dioxin-6-yl)-2-methylphenyl)-5-(((2-hydroxyethyl)amino)methyl)-*N*-methylpicolinamide **A4**

General procedure D. Yield: 16%; 1H NMR (500 MHz, Chloroform-*d*) δ 8.23 (dd, $J = 2.1, 0.8$ Hz, 1H), 7.51 (dd, $J = 8.0, 2.2$ Hz, 1H), 7.31 (dd, $J = 8.0, 0.9$ Hz, 1H), 7.01–6.94 (m, 3H), 6.82 (d, $J = 8.1$ Hz, 1H), 6.61–6.54 (m, 2H), 4.24 (s, 4H), 3.68 (s, 2H), 3.60 (d, $J = 5.0$ Hz, 2H), 3.37 (s, 3H), 2.65–2.59 (m, 2H), 2.10 (s, 3H). ESI-MS: $m/z = 434$ [M+H] $^+$. HRMS (ESI) for $C_{25}H_{27}N_3O_4$ [M+H] $^+$, calcd: 434.2080, found: 434.2079.

4.1.16. *N*-(3-(2,3-dihydrobenzo[*b*] [1,4]dioxin-6-yl)-2-methylphenyl)-4-(((2-hydroxyethyl)amino)methyl)benzenesulfonamide **A5**

General procedure D. Yield: 16%; 1H NMR (500 MHz, Chloroform-*d*) δ 7.72 (d, $J = 8.0$ Hz, 2H), 7.48 (d, $J = 7.8$ Hz, 2H), 7.24 (d, $J = 7.8$ Hz, 1H), 7.13 (t, $J = 7.8$ Hz, 1H), 7.04 (dd, $J = 7.9, 1.3$ Hz, 1H), 6.85 (d, $J = 8.2$ Hz, 1H), 6.70–6.59 (m, 2H), 4.27 (s, 4H), 3.96 (s, 2H), 3.71 (s, 2H), 2.85 (s, 2H), 1.89 (s, 3H). ESI-MS: $m/z = 455$ [M+H] $^+$. HRMS (ESI) for $C_{24}H_{26}N_2O_5S$ [M+H] $^+$, calcd: 455.1641, found: 455.1697.

4.1.17. 3-(2,3-dihydrobenzo[*b*] [1,4]dioxin-6-yl)-2-methylbenzoic acid **10**

3c (100 mg, 0.35 mmol), LiOH (25 mg, 1.05 mmol), THF (10 mL) and H_2O (5 mL) were added in the flask and stir at room temperature. After TLC monitoring, pH was adjusted to acidity with 2 N HCl, extracted by EA, dried by anhydrous sodium sulfate, and

concentrated to remove the solvent to get 70 mg **10**. The crude product was taken on to the next step without purification. Yield: 74%; ESI-MS: $m/z = 271$ [M+H] $^+$

4.1.18. *N*-(4-(bromomethyl)phenyl)-3-(2,3-dihydrobenzo[*b*] [1,4]dioxin-6-yl)-2-methylbenzamide **11**

General procedure C. Yield: 70%; 1H NMR (500 MHz, Chloroform-*d*) δ 7.88 (d, $J = 8.1$ Hz, 2H), 7.71 (s, 1H), 7.53 (d, $J = 8.3$ Hz, 2H), 7.28 (t, $J = 7.9$ Hz, 1H), 7.11 (dd, $J = 7.6, 1.3$ Hz, 1H), 6.91 (d, $J = 8.2$ Hz, 1H), 6.82 (d, $J = 2.1$ Hz, 1H), 6.77 (dd, $J = 8.2, 2.1$ Hz, 1H), 4.54 (s, 2H), 4.31 (s, 4H), 2.23 (s, 3H). ESI-MS: $m/z = 440$ [M+H] $^+$.

4.1.19. 3-(2,3-dihydrobenzo[*b*] [1,4]dioxin-6-yl)-*N*-(4-(((2-hydroxyethyl)amino)methyl)phenyl)-2-methylbenzamide **A6**

General procedure E. Yield: 23%; 1H NMR (500 MHz, Chloroform-*d*) δ 9.04 (s, 1H), 7.93 (d, $J = 7.8$ Hz, 2H), 7.68 (d, $J = 8.1$ Hz, 2H), 7.44 (d, $J = 8.0$ Hz, 1H), 7.19 (t, $J = 7.8$ Hz, 1H), 7.08 (dd, $J = 7.7, 1.4$ Hz, 1H), 6.83 (d, $J = 8.2$ Hz, 1H), 6.76 (d, $J = 2.1$ Hz, 1H), 6.71 (dd, $J = 8.2, 2.1$ Hz, 1H), 4.24 (s, 4H), 3.89–3.86 (m, 2H), 3.69 (s, 2H), 3.12 (dd, $J = 6.0, 4.4$ Hz, 2H), 2.15 (s, 3H). ESI-MS: $m/z = 419$ [M+H] $^+$. HRMS (ESI) for $C_{25}H_{26}N_2O_4$ [M+H] $^+$, calcd: 419.1971, found: 419.1969.

4.1.20. 4-(1-((3-(2,3-dihydrobenzo[*b*] [1,4]dioxin-6-yl)-2-methylphenyl)amino)-2,2,2-trifluoroethyl)benzaldehyde **13**

3b (100 mg, 0.4 mmol), 4-(diethoxymethyl)benzaldehyde (**12**, 86 mg, 0.4 mmol), EtOH (5 mL) were added into the flask and heated to reflux. After TLC monitoring, remove EtOH and add anhydrous THF (10 mL), TBAT (33 mg) and join $TMSCF_3$ (89 mg), stir 2 h at room temperature under nitrogen atmosphere, add 2 N HCl 12 mL, stirring at room temperature for another 1 h. After extraction with ethyl acetate, 130 mg **13** was obtained by column chromatography. Yield: 73%; 1H NMR (500 MHz, Chloroform-*d*) δ 10.04 (s, 1H), 7.94 (d, $J = 8.3$ Hz, 2H), 7.70 (d, $J = 8.0$ Hz, 2H), 7.00 (t, $J = 7.9$ Hz, 1H), 6.89 (d, $J = 8.2$ Hz, 1H), 6.80 (d, $J = 2.0$ Hz, 1H), 6.75 (dd, $J = 8.2, 2.1$ Hz, 1H), 6.72 (dd, $J = 7.7, 1.1$ Hz, 1H), 6.39–6.36 (m, 1H), 5.07 (q, $J = 7.1$ Hz, 1H), 4.30 (s, 4H), 4.30 (s, 2H), 2.18 (s, 3H). ESI-MS: $m/z = 428$ [M+H] $^+$.

4.1.21. 2-((4-(1-((3-(2,3-dihydrobenzo[*b*] [1,4]dioxin-6-yl)-2-methylphenyl)amino)-2,2,2-trifluoroethyl)benzyl)amino)ethan-1-ol **A7**

General procedure D. Yield: 35%; 1H NMR (500 MHz, Chloroform-*d*) δ 7.57 (d, $J = 7.4$ Hz, 2H), 7.52 (d, $J = 8.6$ Hz, 2H), 6.97 (t, $J = 7.9$ Hz, 1H), 6.86 (d, $J = 8.2$ Hz, 1H), 6.80–6.74 (m, 1H), 6.74–6.62 (m, 2H), 6.40 (d, $J = 8.1$ Hz, 1H), 5.08–4.96 (m, 1H), 4.36 (d, $J = 7.0$ Hz, 1H), 4.25 (s, 4H), 4.24 (s, 2H), 3.88 (s, 2H), 3.13 (s, 2H), 2.14 (s, 2H). ESI-MS: $m/z = 473$ [M+H] $^+$. HRMS (ESI) for $C_{26}H_{27}F_3N_2O_3$ [M+H] $^+$, calcd: 473.2052, found: 473.2073.

4.1.22. 4-(2-aminopyridin-4-yl)benzaldehyde **15a**

5 (200 mg, 0.862 mmol), 4-bromo-2-pyridinamine (**14a**, 136 mg, 0.783 mmol), $Pd(PPh_3)_4$ (91 mg, 0.0783 mmol) and 3 mL 2 M K_2CO_3 were added into the flask. Then 5 mL tetrahydrofuran were added. The mixture was heated to reflux overnight under a nitrogen atmosphere. After TLC monitoring, the product was separated and purified by column chromatography (ethyl acetate: petroleum ether = 2:1). 76 mg **15a** was obtained. Yield: 43%; 1H NMR (500 MHz, Chloroform-*d*) δ 10.08 (s, 1H), 8.17 (dd, $J = 5.4, 0.8$ Hz, 1H), 8.00–7.95 (m, 2H), 7.77–7.73 (m, 2H), 6.90 (dd, $J = 5.4, 1.6$ Hz, 1H), 6.74 (dd, $J = 1.6, 0.8$ Hz, 1H), 4.65 (s, 2H). ESI-MS: $m/z = 199$ [M+H] $^+$

4.1.23. 4-(6-aminopyridin-2-yl)benzaldehyde **15b**

Synthesized following a procedure similar to compound **15a**, with the replacement of 4-bromo-2-pyridinamine (**14a**) with 6-

bromo-2-pyridinamine (**14b**) to yield **15b** (75 mg). Yield: 44%; ^1H NMR (500 MHz, Chloroform-*d*) δ 10.06 (s, 1H), 8.15–8.08 (m, 2H), 7.98–7.91 (m, 2H), 7.55 (t, $J = 7.8$ Hz, 1H), 7.17 (d, $J = 7.5$ Hz, 1H), 6.54 (d, $J = 8.1$ Hz, 1H), 4.64 (s, 2H). ESI-MS: $m/z = 199$ [M+H] $^+$

4.1.24. 4-(2-((3-(2,3-dihydrobenzo[*b*] [1,4]dioxin-6-yl)-2-methylphenyl)amino)pyridin-4-yl)benzaldehyde **16a**

15a (75 mg, 0.378 mmol), **3a** (115 mg, 0.378 mmol), Pd(PPh₃)₄ (22 mg, 0.0789 mmol), Xphos (22 mg, 0.0378 mmol) and cesium carbonate (184 mg, 0.568 mmol) were added into the flask. Then 2 mL anhydrous 1, 4-dioxane were added. The mixture was heated to reflux overnight under a nitrogen atmosphere. After TLC monitoring, the product was separated and purified by column chromatography (ethyl acetate: petroleum ether = 1:1), and 80 mg **16a** was obtained. Yield: 50%; ^1H NMR (500 MHz, Chloroform-*d*) δ 10.06 (s, 1H), 8.32–8.23 (m, 1H), 8.00–7.91 (m, 2H), 7.77–7.67 (m, 2H), 7.46 (dd, $J = 7.9$, 1.4 Hz, 1H), 7.27 (s, 0H), 7.24 (d, $J = 7.8$ Hz, 1H), 7.08 (dd, $J = 7.5$, 1.4 Hz, 1H), 6.96 (dd, $J = 5.3$, 1.5 Hz, 1H), 6.94–6.89 (m, 2H), 6.85 (d, $J = 2.1$ Hz, 1H), 6.80 (dd, $J = 8.3$, 2.1 Hz, 1H), 6.55 (s, 1H), 4.31 (s, 4H), 2.23 (s, 3H). ESI-MS: $m/z = 423$ [M+H] $^+$

4.1.25. 4-(6-((3-(2,3-dihydrobenzo[*b*] [1,4]dioxin-6-yl)-2-methylphenyl)amino)pyridin-2-yl)benzaldehyde **16b**

Synthesized following a procedure similar to compound **16a**, with the replacement of **15a** with **15b** to yield **16b** (80 mg). Yield: 50%; ^1H NMR (500 MHz, Chloroform-*d*) δ 10.08 (s, 1H), 8.18 (d, $J = 8.3$ Hz, 2H), 7.98 (d, $J = 8.4$ Hz, 2H), 7.59 (t, $J = 7.9$ Hz, 1H), 7.48 (t, $J = 6.0$ Hz, 2H), 7.25–7.22 (m, 2H), 7.08 (dd, $J = 7.6$, 1.3 Hz, 1H), 6.92 (d, $J = 8.2$ Hz, 1H), 6.86 (d, $J = 2.0$ Hz, 1H), 6.81 (dd, $J = 8.2$, 2.1 Hz, 1H), 6.71 (d, $J = 8.4$ Hz, 1H), 4.31 (s, 4H), 2.23 (s, 3H). ESI-MS: $m/z = 423$ [M+H] $^+$

4.1.26. 2-((4-(2-((3-(2,3-dihydrobenzo[*b*] [1,4]dioxin-6-yl)-2-methylphenyl)amino)pyridin-4-yl)benzyl)amino)ethan-1-ol **A8**

General procedure D. Yield: 18%; ^1H NMR (500 MHz, Methanol-*d*₄) δ 8.05 (d, $J = 4.9$ Hz, 2H), 7.75–7.71 (m, 2H), 7.61–7.57 (m, 2H), 7.33 (dd, $J = 8.0$, 1.3 Hz, 1H), 7.22 (t, $J = 7.7$ Hz, 1H), 7.04 (dd, $J = 7.6$, 1.4 Hz, 1H), 6.98 (dt, $J = 5.5$, 2.0 Hz, 1H), 6.91–6.88 (m, 1H), 6.86 (d, $J = 8.2$ Hz, 1H), 6.79–6.74 (m, 2H), 4.28 (s, 2H), 4.26 (s, 4H), 3.83–3.79 (m, 2H), 3.16–3.12 (m, 2H), 2.14 (s, 3H). ESI-MS: $m/z = 468$ [M+H] $^+$. HRMS (ESI) for C₂₉H₂₉N₃O₃ [M+H] $^+$, calcd: 468.2287, found: 468.2286.

4.1.27. 2-((4-(6-((3-(2,3-dihydrobenzo[*b*] [1,4]dioxin-6-yl)-2-methylphenyl)amino)pyridin-2-yl)benzyl)amino)ethan-1-ol **A9**

General procedure D. Yield: 20%; ^1H NMR (500 MHz, Chloroform-*d*) δ 8.00–7.91 (m, 2H), 7.52 (t, $J = 7.9$ Hz, 1H), 7.50–7.44 (m, 3H), 7.22 (d, $J = 7.8$ Hz, 1H), 7.12 (d, $J = 7.5$ Hz, 1H), 7.05 (dd, $J = 7.6$, 1.4 Hz, 1H), 6.91 (d, $J = 8.2$ Hz, 1H), 6.85 (d, $J = 2.0$ Hz, 1H), 6.80 (dd, $J = 8.2$, 2.0 Hz, 1H), 6.63 (d, $J = 8.3$ Hz, 1H), 6.46 (s, 1H), 4.30 (s, 4H), 3.95 (s, 2H), 3.73 (s, 2H), 2.88 (s, 2H), 2.21 (s, 3H). ESI-MS: $m/z = 468$ [M+H] $^+$. HRMS (ESI) for C₂₉H₂₉N₃O₃ [M+H] $^+$, calcd: 468.2287, found: 468.2287.

4.1.28. 4-(2,3-dihydrobenzo[*b*] [1,4]dioxin-6-yl)-1H-indole **18a**

General procedure A. Yield: 88%; ESI-MS: $m/z = 252$ [M+H] $^+$

4.1.29. 4-(2,3-dihydrobenzo[*b*] [1,4]dioxin-6-yl)indoline **18b**

General procedure A. Yield: 85%; ^1H NMR (500 MHz, DMSO-*d*₆) δ 6.95 (t, $J = 7.7$ Hz, 1H), 6.92–6.88 (m, 3H), 6.53 (dd, $J = 7.6$, 1.0 Hz, 1H), 6.47 (dd, $J = 7.7$, 0.9 Hz, 1H), 5.55 (d, $J = 2.1$ Hz, 1H), 4.26 (s, 4H), 3.38 (dd, $J = 8.4$, 1.8 Hz, 2H), 2.95 (t, $J = 8.3$ Hz, 2H). ESI-MS: $m/z = 254$ [M+H] $^+$

4.1.30. 5-(2,3-dihydrobenzo[*b*] [1,4]dioxin-6-yl)-1,2,3,4-tetrahydroquinoline **18c**

General procedure A. Yield: 87%; ^1H NMR (500 MHz, Chloroform-*d*) δ 7.04–6.98 (m, 1H), 6.88 (d, $J = 8.2$ Hz, 1H), 6.85 (d, $J = 2.0$ Hz, 1H), 6.80 (dd, $J = 8.2$, 2.1 Hz, 1H), 6.57 (dd, $J = 7.5$, 1.2 Hz, 1H), 6.51 (dd, $J = 8.1$, 1.2 Hz, 1H), 4.29 (s, 4H), 3.34–3.29 (m, 2H), 2.65 (t, $J = 6.4$ Hz, 2H), 1.89–1.82 (m, 2H). ^{13}C NMR (126 MHz, CDCl₃) δ 143.16, 142.87, 139.67, 133.86, 129.18, 128.75, 126.26, 125.38, 124.92, 122.48, 118.16, 117.02, 77.27, 77.22, 77.01, 76.76, 64.44, 32.60, 24.88, 24.45. ESI-MS: $m/z = 268$ [M+H] $^+$.

4.1. 31(4-(bromomethyl)phenyl) (4-(2,3-dihydrobenzo[*b*] [1,4]dioxin-6-yl)-1H-indol-1-yl)methanone **19a**

General procedure F. Yield: 90%; ^1H NMR (500 MHz, DMSO-*d*₆) δ 8.30–8.26 (m, 1H), 7.77 (d, 2H), 7.67 (d, 2H), 7.45–7.41 (m, 2H), 7.34 (dd, $J = 7.5$, 1.0 Hz, 1H), 7.07 (dq, $J = 4.6$, 2.1 Hz, 2H), 7.00 (d, $J = 8.8$ Hz, 1H), 6.76 (dd, $J = 3.9$, 0.7 Hz, 1H), 4.82 (s, 2H), 4.30 (s, 4H). ESI-MS: $m/z = 448$ [M+H] $^+$.

4.1.32. (4-(bromomethyl)phenyl) (4-(2,3-dihydrobenzo[*b*] [1,4]dioxin-6-yl)indolin-1-yl)methanone **19b**

General procedure F. Yield: 87%; ESI-MS: $m/z = 450$ [M+H] $^+$.

4.1.33. (4-(bromomethyl)phenyl) (5-(2,3-dihydrobenzo[*b*] [1,4]dioxin-6-yl)-3,4-dihydroquinolin-1(2H)-yl)methanone **19c**

General procedure F. Yield: 77%; ^1H NMR (500 MHz, Chloroform-*d*) δ 7.35 (d, $J = 8.2$ Hz, 2H), 7.30 (d, $J = 7.6$ Hz, 2H), 6.99 (dd, $J = 7.6$, 0.9 Hz, 1H), 6.93 (d, $J = 8.2$ Hz, 1H), 6.90 (t, $J = 7.8$ Hz, 1H), 6.85 (d, $J = 2.0$ Hz, 1H), 6.81 (dd, $J = 8.2$, 2.0 Hz, 1H), 6.64 (s, 1H), 4.44 (s, 2H), 4.32 (s, 4H), 3.89 (t, $J = 6.8$ Hz, 2H), 2.75 (t, $J = 6.2$ Hz, 2H), 1.95 (t, $J = 6.5$ Hz, 2H). ESI-MS: $m/z = 465$ [M+H] $^+$.

4.1.34. (4-(2,3-dihydrobenzo[*b*] [1,4]dioxin-6-yl)-1H-indol-1-yl) (4-(((2-hydroxyethyl)amino)methyl)phenyl)methanone **A10**

General procedure E. Yield: 21%; HPLC: t_R 13.301 min, purity 95.71%. ^1H NMR (500 MHz, DMSO-*d*₆) δ 8.26 (d, $J = 8.2$ Hz, 1H), 7.74 (d, $J = 8.0$ Hz, 2H), 7.58 (d, $J = 7.8$ Hz, 2H), 7.45–7.40 (m, 2H), 7.33 (d, $J = 7.4$ Hz, 1H), 7.07 (dq, $J = 4.6$, 2.2 Hz, 2H), 7.00 (d, $J = 8.8$ Hz, 1H), 6.77 (d, $J = 3.9$ Hz, 1H), 4.30 (s, 4H), 3.89 (s, 2H), 3.52 (t, $J = 5.8$ Hz, 2H), 2.65 (t, $J = 5.7$ Hz, 2H). ESI-MS: $m/z = 429$ [M+H] $^+$.

4.1.35. (4-(2,3-dihydrobenzo[*b*] [1,4]dioxin-6-yl)indolin-1-yl) (4-(((2-hydroxyethyl)amino)methyl)phenyl)methanone **A11**

General procedure E. Yield: 22%; ^1H NMR (500 MHz, DMSO-*d*₆) δ 7.52 (d, $J = 7.7$ Hz, 2H), 7.44 (d, $J = 7.9$ Hz, 2H), 7.23 (s, 1H), 7.11–6.77 (m, 5H), 4.52 (s, 1H), 4.26 (s, 4H), 3.98 (t, $J = 8.1$ Hz, 2H), 3.77 (s, 2H), 3.48 (t, $J = 5.8$ Hz, 2H), 3.10 (t, $J = 8.1$ Hz, 2H), 2.58 (t, $J = 5.8$ Hz, 2H). ESI-MS: $m/z = 431$ [M+H] $^+$.

4.1.36. (5-(2,3-dihydrobenzo[*b*] [1,4]dioxin-6-yl)-3,4-dihydroquinolin-1(2H)-yl) (4-(((2-hydroxyethyl)amino)methyl)phenyl)methanone **A12**

General procedure E. Yield: 24%; HPLC: t_R 13.303 min, purity 96.26%. ^1H NMR (500 MHz, Chloroform-*d*) δ 7.34 (d, $J = 7.9$ Hz, 2H), 7.27 (s, 1H), 7.25 (s, 1H), 6.97 (dd, $J = 7.6$, 1.2 Hz, 1H), 6.92 (d, $J = 8.2$ Hz, 1H), 6.89–6.83 (m, 2H), 6.80 (dd, $J = 8.2$, 2.1 Hz, 1H), 6.63 (s, 1H), 4.31 (s, 4H), 3.88 (t, $J = 7.0$ Hz, 2H), 3.83 (s, 2H), 3.66 (t, $J = 5.1$ Hz, 2H), 2.79 (t, $J = 5.1$ Hz, 2H), 2.75 (t, $J = 6.4$ Hz, 2H), 1.95 (q, $J = 6.7$ Hz, 2H). ^{13}C NMR (126 MHz, CDCl₃) δ 168.95, 142.14, 141.84, 139.74, 138.48, 135.10, 132.82, 128.08, 127.70, 125.26, 124.31, 123.87, 121.48, 117.15, 115.99, 76.24, 76.19, 75.99, 75.73, 63.41, 51.14, 48.84, 28.68, 23.83, 23.41. ESI-MS: $m/z = 445$ [M+H] $^+$.

4.1.37. 5-vinylisoindolin-1-one **21**

A solution of 5-bromo-2,3-dihydro-1H-isoindol-1-one (**20**,

200 mg, 0.94 mmol), tributyl (vinyl)tin (419 mg, 1.32 mmol), and Pd[P(Ph)₃]₄ (54 mg, 0.047 mmol) in toluene (5 mL) was refluxed under a nitrogen atmosphere. After TLC monitoring, the reaction mixture was purified by column chromatography using silica gel to yield **20** (116 mg). Yield: 77%; ¹H NMR (500 MHz, DMSO-*d*₆) δ 7.83 (d, *J* = 1.5 Hz, 1H), 7.69–7.65 (m, 2H), 6.85 (dd, *J* = 17.6, 10.9 Hz, 1H), 5.97 (dd, *J* = 17.6, 0.9 Hz, 1H), 5.38 (dd, *J* = 10.9, 0.8 Hz, 1H), 4.37 (s, 2H). ESI-MS: *m/z* = 160 [M+H]⁺.

4.1.38. 2-(3-(2,3-dihydrobenzo[*b*] [1,4]dioxin-6-yl)-2-methylphenyl)-5-vinylisoindolin-1-one **22**

3a (222 mg, 0.729 mmol), **21** (116 mg, 0.729 mmol), CuI (28 mg, 0.146 mmol), Cs₂CO₃ (474 mg, 1.46 mmol) and DMCHDA (CAS: 87583-89-9) (31 mg, 0.219 mmol) were dissolved in toluene (5 mL). After TLC monitoring, the reaction mixture was purified by column chromatography using silica gel to yield **22** (100 mg). Yield: 36%; ¹H NMR (500 MHz, DMSO-*d*₆) δ 7.77 (s, 1H), 7.73 (d, *J* = 5.2 Hz, 1H), 7.66 (dd, *J* = 8.0, 1.4 Hz, 1H), 7.40 (dd, *J* = 7.8, 1.4 Hz, 1H), 7.33 (t, *J* = 7.7 Hz, 1H), 7.23 (dd, *J* = 7.6, 1.6 Hz, 1H), 6.93 (d, *J* = 0.9 Hz, 1H), 6.92–6.85 (m, 1H), 6.82 (d, *J* = 2.0 Hz, 1H), 6.80 (dd, *J* = 8.2, 2.1 Hz, 1H), 6.03 (dd, *J* = 17.6, 0.8 Hz, 1H), 5.43 (d, *J* = 11.4 Hz, 1H), 4.28 (s, 6H), 2.03 (s, 3H). ESI-MS: *m/z* = 384 [M+H]⁺

4.1.39. 2-(3-(2,3-dihydrobenzo[*b*] [1,4]dioxin-6-yl)-2-methylphenyl)-1-oxoisindoline-5-carbaldehyde **23**

General procedure G. Yield: 33%; ¹H NMR (500 MHz, DMSO-*d*₆) δ 10.19 (s, 1H), 8.20 (q, *J* = 2.5, 1.8 Hz, 1H), 8.10 (dd, *J* = 7.8, 1.3 Hz, 1H), 8.00 (d, *J* = 7.8 Hz, 1H), 7.43 (dd, *J* = 7.9, 1.4 Hz, 1H), 7.36 (t, *J* = 7.7 Hz, 1H), 7.26 (dd, *J* = 7.6, 1.4 Hz, 1H), 6.95 (d, *J* = 8.2 Hz, 1H), 6.86–6.77 (m, 2H), 4.99 (s, 2H), 4.29 (s, 4H), 2.04 (s, 3H). ESI-MS: *m/z* = 386 [M+H]⁺

4.1.40. 2-(3-(2,3-dihydrobenzo[*b*] [1,4]dioxin-6-yl)-2-methylphenyl)-5-(((2-hydroxyethyl)amino)methyl)isoindolin-1-one **B1**

General procedure D. Yield: 15%; ¹H NMR (500 MHz, DMSO-*d*₆) δ 7.77 (d, *J* = 7.7 Hz, 1H), 7.68 (s, 1H), 7.58 (d, *J* = 7.9 Hz, 1H), 7.40 (d, *J* = 7.8 Hz, 1H), 7.34 (t, *J* = 7.6 Hz, 1H), 7.23 (d, *J* = 7.7 Hz, 1H), 6.94 (d, *J* = 8.2 Hz, 1H), 6.84–6.77 (m, 2H), 4.88 (s, 2H), 4.28 (s, 4H), 3.56 (s, 2H), 2.75 (s, 1H), 2.65–2.62 (m, 2H), 2.36 (p, *J* = 1.9 Hz, 2H), 2.03 (s, 3H). ESI-MS: *m/z* = 431 [M+H]⁺. HRMS (ESI) for C₂₆H₂₆N₂O₄ [M+H]⁺, calcd: 431.1971, found: 431.1966.

4.1.41. 1-(2-chloroethyl)-3-(3-(2,3-dihydrobenzo[*b*] [1,4]dioxin-6-yl)-2-methylphenyl)urea **24**

To a solution of **3b** (300 mg, 1.243 mmol) in DCM (10 mL) and 2-Chloroethyl isocyanate (157 mg, 1.49 mmol) were added in 0 °C and the reaction was allowed to stir overnight at room temperature. The reaction mixture was concentrated under vacuum and the resulting crude product was taken as such to the next step without further purification. Yield: 100%; ¹H NMR (500 MHz, DMSO-*d*₆) δ 7.88 (s, 1H), 7.72 (d, *J* = 8.0 Hz, 1H), 7.11 (t, *J* = 7.8 Hz, 1H), 6.90 (d, *J* = 8.2 Hz, 1H), 6.87–6.80 (m, 2H), 6.78–6.70 (m, 2H), 4.27 (s, 4H), 3.67 (t, *J* = 6.1 Hz, 2H), 3.43 (q, *J* = 5.9 Hz, 2H), 2.06 (s, 3H). ESI-MS: *m/z* = 347 [M+H]⁺.

4.1.42. 1-(3-(2,3-dihydrobenzo[*b*] [1,4]dioxin-6-yl)-2-methylphenyl)imidazolidin-2-one **25**

To a solution of **24** (343 mg, 0.989 mmol) in THF (6 mL) and NaH (119 mg, 2.967 mmol) were added in 0 °C under a nitrogen atmosphere. The reaction was allowed to stir at room temperature for 4 h. After TLC monitoring, the solution was quenched by adding NH₄Cl, and extracted by DCM, dried over sodium sulfate, and concentrated under vacuum to yield **25** as solid (250 mg), which was taken as such to the next step without further purification.

Yield: 82%; ¹H NMR (500 MHz, DMSO-*d*₆) δ 7.25–7.18 (m, 2H), 7.08 (dd, *J* = 7.3, 1.6 Hz, 1H), 6.92 (d, *J* = 8.2 Hz, 1H), 6.78 (d, *J* = 2.0 Hz, 1H), 6.75 (dd, *J* = 8.2, 2.1 Hz, 1H), 6.66 (s, 1H), 4.28 (s, 4H), 3.73 (dd, *J* = 8.9, 6.6 Hz, 2H), 3.43 (ddd, *J* = 9.2, 6.5, 1.1 Hz, 2H), 2.09 (s, 3H). ESI-MS: *m/z* = 310 [M+H]⁺.

4.1.43. 1-(3-(2,3-dihydrobenzo[*b*] [1,4]dioxin-6-yl)-2-methylphenyl)-3-(4-(((2-hydroxyethyl)amino)methyl)phenyl)imidazolidin-2-one **B2**

General procedure G. Yield: 30%; HPLC: t_R 13.343 min, purity 96.94%. ¹H NMR (500 MHz, Chloroform-*d*) δ 7.61–7.55 (m, 2H), 7.33 (d, *J* = 8.3 Hz, 2H), 7.28 (d, *J* = 7.9 Hz, 1H), 7.26–7.23 (m, 1H), 7.20–7.17 (m, 1H), 6.89 (d, *J* = 8.2 Hz, 1H), 6.85 (d, *J* = 2.0 Hz, 1H), 6.80 (dd, *J* = 8.3, 2.1 Hz, 1H), 4.29 (s, 4H), 4.01 (dd, *J* = 9.3, 6.5 Hz, 2H), 3.91–3.86 (m, 2H), 3.81 (s, 2H), 3.68 (t, *J* = 5.1 Hz, 2H), 2.83 (t, *J* = 5.1 Hz, 2H), 2.21 (s, 3H). ESI-MS: *m/z* = 460 [M+H]⁺. HRMS (ESI) for C₂₇H₂₉N₃O₄ [M+H]⁺, calcd: 460.2236, found: 460.2239.

4.1.44. 1-(3-(2,3-dihydrobenzo[*b*] [1,4]dioxin-6-yl)-2-methylphenyl)-3-(5-(((2-hydroxyethyl)amino)methyl)pyridin-2-yl)imidazolidin-2-one **B3**

General procedure G. Yield: 15%; ¹H NMR (500 MHz, Chloroform-*d*) δ 8.27 (d, *J* = 2.5 Hz, 2H), 8.22 (d, *J* = 8.5 Hz, 1H), 7.56 (dd, *J* = 8.2, 2.5 Hz, 1H), 7.45 (t, *J* = 8.6 Hz, 2H), 7.24–7.21 (m, 1H), 7.21–7.16 (m, 1H), 6.87 (d, *J* = 8.2 Hz, 1H), 6.81 (d, *J* = 2.0 Hz, 1H), 6.76 (d, *J* = 8.4 Hz, 1H), 4.27 (s, 4H), 4.26 (s, 2H), 4.21 (dd, *J* = 9.1, 7.2 Hz, 2H), 3.86 (t, *J* = 8.1 Hz, 2H), 3.64 (d, *J* = 5.1 Hz, 2H), 2.72 (s, 2H), 2.17 (s, 3H). ESI-MS: *m/z* = 461 [M+H]⁺. HRMS (ESI) for C₂₆H₂₈N₄O₄ [M+H]⁺, calcd: 461.2189, found: 461.2181.

4.1.45. 1-(3-(2,3-dihydrobenzo[*b*] [1,4]dioxin-6-yl)-2-methylphenyl)-3-(3-(((2-hydroxyethyl)amino)methyl)phenyl)imidazolidin-2-one **B4**

General procedure G. Yield: 17%; HPLC: t_R 13.353 min, purity 97.34%. ¹H NMR (500 MHz, DMSO-*d*₆) δ 7.66 (s, 1H), 7.59 (d, *J* = 8.7 Hz, 2H), 7.35 (d, *J* = 7.5 Hz, 1H), 7.34–7.27 (m, 3H), 7.16 (dd, *J* = 7.3, 1.7 Hz, 1H), 6.93 (d, *J* = 8.1 Hz, 1H), 6.82–6.75 (m, 2H), 4.28 (s, 4H), 4.04–3.97 (m, 2H), 3.93 (s, 2H), 3.88 (dd, *J* = 9.3, 6.5 Hz, 2H), 3.55 (d, *J* = 5.5 Hz, 2H), 3.50 (td, *J* = 5.9, 3.0 Hz, 2H), 2.12 (s, 3H). ESI-MS: *m/z* = 460 [M+H]⁺. HRMS (ESI) for C₂₇H₂₉N₃O₄ [M+H]⁺, calcd: 460.2236, found: 460.2228.

4.1.46. 1-(3-(2,3-dihydrobenzo[*b*] [1,4]dioxin-6-yl)-2-methylphenyl)-3-(6-(((2-hydroxyethyl)amino)methyl)pyridin-2-yl)imidazolidin-2-one **B5**

General procedure G. Yield: 21%; HPLC: t_R 13.162 min, purity 97.53%. ¹H NMR (500 MHz, Chloroform-*d*) δ 8.36 (s, 1H), 7.65 (t, *J* = 8.0 Hz, 1H), 7.22 (d, *J* = 9.8 Hz, 2H), 6.96–6.87 (m, 2H), 6.86–6.82 (m, 1H), 6.81–6.76 (m, 1H), 4.41 (s, 2H), 4.29 (s, 4H), 4.27 (s, 2H), 3.97 (s, 2H), 3.88 (s, 2H), 3.15 (s, 2H), 2.19 (s, 3H). ESI-MS: *m/z* = 461 [M+H]⁺. HRMS (ESI) for C₂₆H₂₈N₄O₄ [M+H]⁺, calcd: 461.2189, found: 461.2218.

4.1.47. 1-(3-(2,3-dihydrobenzo[*b*] [1,4]dioxin-6-yl)-2-methylphenyl)-3-(4-(((2-hydroxyethyl)amino)methyl)thiazol-2-yl)imidazolidin-2-one **B6**

General procedure G. Yield: 26%; ¹H NMR (500 MHz, DMSO-*d*₆) δ 7.39–7.29 (m, 3H), 7.20 (dd, *J* = 7.6, 1.5 Hz, 1H), 6.93 (d, *J* = 8.2 Hz, 1H), 6.81 (d, *J* = 2.1 Hz, 1H), 6.78 (dd, *J* = 8.2, 2.1 Hz, 1H), 4.28 (s, 4H), 4.21 (dd, *J* = 9.2, 6.8 Hz, 2H), 4.16 (s, 2H), 3.99 (t, *J* = 8.1 Hz, 2H), 3.68 (q, *J* = 5.3 Hz, 2H), 3.02 (t, *J* = 5.5 Hz, 2H), 2.12 (s, 3H). ESI-MS: *m/z* = 467 [M+H]⁺. HRMS (ESI) for C₂₄H₂₆N₄O₄S [M+H]⁺, calcd: 467.1753, found: 467.1755.

4.1.48. 3-(2,3-dihydrobenzo[b][1,4]dioxin-6-yl)-2-methylbenzohydrazide **28**

A solution of **3c** (1 g, 3.5 mmol), hydrated hydrazine (1.4 g, 35 mmol) in ethanol (10 mL) was refluxed. After TLC monitoring, the reaction mixture was purified by column chromatography using silica gel to yield **28** (464 mg). Yield: 46.4%; ¹H NMR (500 MHz, DMSO-*d*₆) δ 9.44 (s, 1H), 7.27–7.19 (m, 3H), 6.92 (d, *J* = 8.2 Hz, 1H), 6.77 (d, *J* = 2.1 Hz, 1H), 6.74 (dd, *J* = 8.2, 2.1 Hz, 1H), 4.55 (s, 2H), 4.28 (s, 4H), 2.17 (s, 3H). ¹³C NMR (126 MHz, CDCl₃) δ 168.51, 142.62, 142.25, 141.33, 136.85, 133.75, 132.13, 130.12, 125.73, 125.03, 121.64, 117.24, 116.50, 63.74, 63.73, 39.74, 39.65, 39.57, 39.48, 39.41, 39.32, 39.24, 39.15, 39.07, 38.98, 38.89, 38.81, 38.65, 16.98. ESI-MS: *m/z* = 285 [M+H]⁺.

4.1.49. *N'*-(4-(bromomethyl)benzoyl)-3-(2,3-dihydrobenzo[b][1,4]dioxin-6-yl)-2-methylbenzohydrazide **29**

General procedure F. Yield: 30%; ¹H NMR (500 MHz, DMSO-*d*₆) δ 10.57 (d, *J* = 1.3 Hz, 1H), 10.26 (d, *J* = 1.3 Hz, 1H), 7.92 (d, *J* = 8.3 Hz, 2H), 7.59 (d, *J* = 8.3 Hz, 2H), 7.38 (dd, *J* = 7.5, 1.6 Hz, 1H), 7.33 (t, *J* = 7.5 Hz, 1H), 7.28 (dd, *J* = 7.6, 1.7 Hz, 1H), 6.94 (d, *J* = 8.2 Hz, 1H), 6.81 (d, *J* = 2.0 Hz, 1H), 6.78 (dd, *J* = 8.1, 2.1 Hz, 1H), 4.77 (s, 2H), 4.29 (s, 4H), 2.30 (s, 3H). ¹³C NMR (126 MHz, DMSO) δ 169.41, 166.01, 147.11, 143.48, 143.13, 142.36, 136.92, 134.45, 133.28, 131.45, 131.25, 127.83, 126.63, 126.60, 126.00, 122.49, 118.09, 117.37, 64.57, 62.88, 40.55, 40.46, 40.39, 40.29, 40.22, 40.13, 40.05, 39.96, 39.88, 39.79, 39.63, 39.46, 17.84.

4.1.50. 2-(4-(bromomethyl)phenyl)-5-(3-(2,3-dihydrobenzo[b][1,4]dioxin-6-yl)-2-methylphenyl)-1,3,4-oxadiazole **30**

A solution of **29** (100 mg, 0.208 mmol) and POCl₃ (10 mL) was refluxed for 6 h. After TLC monitoring, the solvent was evaporated under vacuum, and the resulting crude product was purified by column chromatography using silica gel to yield **30** (80 mg). Yield: 83%; ¹H NMR (500 MHz, Chloroform-*d*) δ 8.13 (d, *J* = 8.1 Hz, 2H), 7.96 (dd, *J* = 7.6, 1.7 Hz, 1H), 7.57 (d, *J* = 7.8 Hz, 2H), 7.44–7.35 (m, 2H), 6.94 (d, *J* = 8.2 Hz, 1H), 6.86 (d, *J* = 2.1 Hz, 1H), 6.80 (dd, *J* = 8.2, 2.1 Hz, 1H), 4.55 (s, 2H), 4.32 (s, 4H), 2.61 (s, 3H). ¹³C NMR (126 MHz, CDCl₃) δ 143.57, 143.17, 142.92, 141.44, 136.24, 134.58, 133.09, 130.67, 129.79, 129.27, 129.14, 128.44, 127.38, 125.78, 123.92, 122.51, 118.22, 117.04, 77.27, 77.22, 77.01, 76.76, 64.44, 32.30, 19.23.

4.1.51. 2-(((4-(5-(3-(2,3-dihydrobenzo[b][1,4]dioxin-6-yl)-2-methylphenyl)-1,3,4-oxadiazol-2-yl)benzyl)amino)ethan-1-ol **B7**

General procedure D. Yield: 62.68%; HPLC: *t*_R 14.430 min, purity 95.27%. ¹H NMR (500 MHz, Chloroform-*d*) δ 8.11 (d, *J* = 8.0 Hz, 2H), 7.95 (dd, *J* = 7.5, 1.8 Hz, 1H), 7.54 (d, *J* = 7.9 Hz, 2H), 7.42–7.34 (m, 2H), 6.94 (d, *J* = 8.2 Hz, 1H), 6.85 (d, *J* = 2.1 Hz, 1H), 6.80 (dd, *J* = 8.2, 2.1 Hz, 1H), 4.32 (s, 4H), 3.95 (s, 2H), 3.73 (t, *J* = 5.1 Hz, 2H), 2.87 (t, *J* = 5.1 Hz, 2H), 2.61 (s, 3H). ¹³C NMR (126 MHz, CDCl₃) δ 165.15, 164.14, 143.52, 143.16, 142.92, 142.90, 136.18, 134.60, 133.00, 129.00, 128.40, 127.16, 125.75, 123.99, 123.03, 122.51, 118.22, 117.03, 77.27, 77.22, 77.02, 76.76, 64.43, 60.60, 52.89, 50.42, 19.23. ESI-MS: *m/z* = 444 [M+H]⁺. HRMS (ESI) for C₂₆H₂₅N₃O₄ [M+H]⁺, calcd: 444.1923, found: 444.1922.

4.1.52. 2-(3-(2,3-dihydrobenzo[b][1,4]dioxin-6-yl)-2-methylphenyl)-4,4,5,5-tetramethyl-1,3,2-dioxaborolane **31**

General procedure B. Yield: 83%; ¹H NMR (500 MHz, Chloroform-*d*) δ 7.73 (dd, *J* = 7.3, 1.7 Hz, 1H), 7.25 (d, *J* = 1.6 Hz, 1H), 7.20 (t, *J* = 7.4 Hz, 1H), 6.89 (d, *J* = 8.2 Hz, 1H), 6.80 (d, *J* = 2.1 Hz, 1H), 6.75 (dd, *J* = 8.2, 2.1 Hz, 1H), 4.30 (s, 4H), 2.43 (s, 3H), 1.36 (s, 12H). ¹³C NMR (126 MHz, CDCl₃) δ 143.09, 142.52, 141.93, 141.78, 136.17, 134.90, 132.65, 124.84, 122.69, 118.32, 116.86, 83.69, 64.56, 25.02, 20.01. ESI-MS: *m/z* = 353 [M+H]⁺.

4.1.53. 6-(3-(2,3-dihydrobenzo[b][1,4]dioxin-6-yl)-2-methylphenyl)nicotinaldehyde **32a**

General procedure H. Yield: 38%; ¹H NMR (500 MHz, DMSO-*d*₆) δ 10.16 (s, 1H), 9.17 (dd, *J* = 2.2, 0.9 Hz, 1H), 8.32 (dd, *J* = 8.1, 2.2 Hz, 1H), 7.79 (dt, *J* = 8.0, 0.6 Hz, 1H), 7.38 (dd, *J* = 7.6, 1.8 Hz, 1H), 7.35 (t, *J* = 7.5 Hz, 1H), 7.28 (dd, *J* = 7.3, 1.8 Hz, 1H), 6.93 (d, *J* = 8.2 Hz, 1H), 6.85 (d, *J* = 2.1 Hz, 1H), 6.82 (dd, *J* = 8.2, 2.1 Hz, 1H), 4.28 (s, 4H), 2.14 (s, 3H). ESI-MS: *m/z* = 332 [M+H]⁺.

4.1.54. 3'-(2,3-dihydrobenzo[b][1,4]dioxin-6-yl)-2'-methyl-[1,1'-biphenyl]-4-carbaldehyde **32b**

General procedure G. Yield: 45%; ¹H NMR (500 MHz, Chloroform-*d*) δ 10.07 (s, 1H), 7.99–7.92 (m, 2H), 7.58–7.50 (m, 2H), 7.31–7.27 (m, 1H), 7.27 (d, *J* = 1.9 Hz, 1H), 7.20 (dd, *J* = 7.2, 1.9 Hz, 1H), 6.92 (d, *J* = 8.2 Hz, 1H), 6.88 (d, *J* = 2.0 Hz, 1H), 6.83 (dt, *J* = 8.2, 2.5 Hz, 1H), 4.31 (s, 4H), 2.12 (s, 3H). ¹³C NMR (126 MHz, CDCl₃) δ 192.02, 148.98, 143.08, 142.69, 142.60, 141.51, 135.37, 134.94, 132.82, 130.11, 129.79, 129.60, 128.45, 125.51, 122.48, 118.16, 116.92, 77.27, 77.22, 77.01, 76.76, 64.44, 64.42, 18.73. ESI-MS: *m/z* = 331 [M+H]⁺.

4.1.55. 3'-(2,3-dihydrobenzo[b][1,4]dioxin-6-yl)-3-methoxy-2'-methyl-[1,1'-biphenyl]-4-carbaldehyde **32c**

General procedure G. Yield: 45%; ¹H NMR (500 MHz, Chloroform-*d*) δ 10.50 (s, 1H), 7.88 (d, *J* = 7.9 Hz, 1H), 7.31–7.26 (m, 2H), 7.20 (dd, *J* = 7.1, 2.0 Hz, 1H), 7.03 (dt, *J* = 7.9, 1.0 Hz, 1H), 6.97 (d, *J* = 1.3 Hz, 1H), 6.92 (d, *J* = 8.2 Hz, 1H), 6.87 (d, *J* = 2.0 Hz, 1H), 6.82 (dd, *J* = 8.2, 2.1 Hz, 1H), 4.31 (s, 4H), 3.95 (s, 3H), 2.13 (s, 3H). ESI-MS: *m/z* = 361 [M+H]⁺.

4.1.56. 2-(((6-(3-(2,3-dihydrobenzo[b][1,4]dioxin-6-yl)-2-methylphenyl)pyridin-3-yl)methyl)amino)ethan-1-ol **B8**

General procedure D. Yield: 43%; ¹H NMR (500 MHz, Chloroform-*d*) δ 8.67 (s, 1H), 7.97 (d, *J* = 8.0 Hz, 1H), 7.49 (d, *J* = 7.9 Hz, 1H), 7.25 (t, *J* = 2.6 Hz, 3H), 6.87 (d, *J* = 8.2 Hz, 1H), 6.81 (d, *J* = 2.1 Hz, 1H), 6.76 (dd, *J* = 8.3, 2.1 Hz, 1H), 5.04 (s, 1H), 4.26 (s, 4H), 4.18 (s, 2H), 3.84 (s, 2H), 2.84 (d, *J* = 5.5 Hz, 2H), 2.10 (s, 3H). ESI-MS: *m/z* = 377 [M+H]⁺.

4.1.57. 2-(((3'-(2,3-dihydrobenzo[b][1,4]dioxin-6-yl)-2'-methyl-[1,1'-biphenyl]-4-yl)methyl)amino)ethan-1-ol **B9**

General procedure D. Yield: 34%; HPLC: *t*_R 14.290 min, purity 95.16%. ¹H NMR (500 MHz, DMSO-*d*₆) δ 7.46 (d, *J* = 7.7 Hz, 2H), 7.36 (d, *J* = 7.8 Hz, 2H), 7.27 (t, *J* = 7.6 Hz, 1H), 7.18–7.13 (m, 2H), 6.91 (d, *J* = 8.2 Hz, 1H), 6.84 (d, *J* = 2.1 Hz, 1H), 6.80 (dd, *J* = 8.3, 2.1 Hz, 1H), 4.26 (s, 4H), 3.95 (s, 2H), 2.84 (t, *J* = 5.3 Hz, 2H), 2.78 (t, *J* = 5.6 Hz, 2H), 2.06 (s, 3H). ESI-MS: *m/z* = 376 [M+H]⁺. HRMS (ESI) for C₂₄H₂₅NO₃ [M+H]⁺, calcd: 376.1913, found: 376.1972.

4.1.58. 2-(((3'-(2,3-dihydrobenzo[b][1,4]dioxin-6-yl)-3-methoxy-2'-methyl-[1,1'-biphenyl]-4-yl)methyl)amino)ethan-1-ol **B10**

General procedure D. Yield: 52%; ¹H NMR (500 MHz, DMSO-*d*₆) δ 7.50 (d, *J* = 7.6 Hz, 1H), 7.29 (t, *J* = 7.6 Hz, 1H), 7.19 (dd, *J* = 7.0, 5.4 Hz, 2H), 7.03 (d, *J* = 1.6 Hz, 1H), 6.96 (dd, *J* = 7.6, 1.5 Hz, 1H), 6.92 (d, *J* = 8.3 Hz, 1H), 6.86 (d, *J* = 2.0 Hz, 1H), 6.82 (dd, *J* = 8.2, 2.1 Hz, 1H), 4.27 (s, 4H), 4.03 (s, 2H), 3.85 (s, 3H), 3.65 (t, *J* = 5.6 Hz, 2H), 2.88 (t, *J* = 5.5 Hz, 2H), 2.09 (s, 3H). ESI-MS: *m/z* = 406 [M+H]⁺. HRMS (ESI) for C₂₅H₂₇NO₄ [M+H]⁺, calcd: 406.2018, found: 406.2022.

4.1.59. 5-(3-(2,3-dihydrobenzo[b][1,4]dioxin-6-yl)-2-methylphenyl)furan-2-carbaldehyde **33a**

General procedure G. Yield: 55%; ¹H NMR (500 MHz, Chloroform-*d*) δ 9.68 (s, 1H), 7.70 (dd, *J* = 7.0, 2.3 Hz, 1H), 7.35 (d, *J* = 3.7 Hz, 1H), 7.29 (d, *J* = 1.9 Hz, 2H), 6.92 (d, *J* = 8.2 Hz, 1H), 6.84 (d,

$J = 2.1$ Hz, 1H), 6.78 (dd, $J = 8.2$, 2.1 Hz, 1H), 6.74 (d, $J = 3.7$ Hz, 1H), 4.31 (s, 4H), 2.38 (s, 3H). ESI-MS: $m/z = 321$ [M+H]⁺.

4.1.60. 5-(3-(2,3-dihydrobenzo[b][1,4]dioxin-6-yl)-2-methylphenyl)thiophene-2-carbaldehyde **33b**

General procedure G. Yield: 63%; ¹H NMR (500 MHz, Chloroform-*d*) δ 9.92 (s, 1H), 7.76 (d, $J = 3.8$ Hz, 1H), 7.36 (dd, $J = 5.8$, 3.4 Hz, 1H), 7.28 (d, $J = 3.4$ Hz, 2H), 7.17 (d, $J = 3.7$ Hz, 1H), 6.92 (d, $J = 8.2$ Hz, 1H), 6.85 (d, $J = 2.0$ Hz, 1H), 6.80 (dd, $J = 8.2$, 2.1 Hz, 1H), 4.31 (s, 4H), 2.27 (s, 3H). ESI-MS: $m/z = 337$ [M+H]⁺

4.1.61. 2-(((5-(3-(2,3-dihydrobenzo[b][1,4]dioxin-6-yl)-2-methylphenyl)furan-2-yl)methyl)amino)ethan-1-ol **B11**

General procedure D. Yield: 80%; ¹H NMR (500 MHz, DMSO-*d*₆) δ 7.57 (dd, $J = 7.8$, 1.4 Hz, 1H), 7.28 (t, $J = 7.7$ Hz, 1H), 7.13 (dd, $J = 7.6$, 1.4 Hz, 1H), 6.92 (d, $J = 8.2$ Hz, 1H), 6.81 (d, $J = 2.1$ Hz, 1H), 6.77 (dd, $J = 8.2$, 2.1 Hz, 1H), 6.61 (d, $J = 3.3$ Hz, 1H), 6.39 (d, $J = 3.2$ Hz, 1H), 4.28 (s, 4H), 3.77 (s, 2H), 3.47 (t, $J = 5.8$ Hz, 2H), 3.17 (s, 1H), 2.63 (t, $J = 5.8$ Hz, 2H), 2.28 (s, 3H). ¹³C NMR (126 MHz, DMSO) δ 154.51, 152.11, 143.42, 143.01, 142.78, 135.09, 132.12, 131.38, 129.40, 126.60, 126.14, 122.61, 118.22, 117.25, 110.68, 109.10, 64.57, 60.69, 51.35, 46.00, 40.55, 40.46, 40.39, 40.29, 40.22, 40.13, 40.05, 39.96, 39.88, 39.79, 39.71, 39.63, 39.46, 19.37. ESI-MS: $m/z = 366$ [M+H]⁺.

4.1.62. 2-(((5-(3-(2,3-dihydrobenzo[b][1,4]dioxin-6-yl)-2-methylphenyl)thiophen-2-yl)methyl)amino)ethan-1-ol **B12**

General procedure D. Yield: 29%; ¹H NMR (500 MHz, DMSO-*d*₆) δ 7.30 (dd, $J = 7.7$, 1.6 Hz, 1H), 7.26 (t, $J = 7.6$ Hz, 1H), 7.16 (dd, $J = 7.5$, 1.6 Hz, 1H), 6.99 (t, $J = 3.2$ Hz, 2H), 6.91 (d, $J = 8.2$ Hz, 1H), 6.83 (d, $J = 2.0$ Hz, 1H), 6.79 (dd, $J = 8.1$, 2.1 Hz, 1H), 4.56 (s, 1H), 4.28 (s, 4H), 3.94 (s, 2H), 3.83 (d, $J = 6.7$ Hz, 1H), 3.49 (q, $J = 5.4$ Hz, 2H), 2.66 (t, $J = 5.8$ Hz, 2H), 2.22 (s, 3H). ¹³C NMR (126 MHz, DMSO) δ 143.42, 143.02, 142.68, 141.63, 135.33, 135.14, 133.49, 129.71, 129.54, 127.11, 126.14, 122.55, 118.17, 117.26, 72.03, 64.57, 60.50, 51.29, 40.57, 40.48, 40.40, 40.31, 40.24, 40.15, 40.07, 39.98, 39.90, 39.81, 39.65, 39.48, 19.34. ESI-MS: $m/z = 382$ [M+H]⁺.

4.1.63. 3'-(2,3-dihydrobenzo[b][1,4]dioxin-6-yl)-3-hydroxy-2'-methyl-[1,1'-biphenyl]-4-carbaldehyde **35**

General procedure G. Yield: 76%; ¹H NMR (500 MHz, DMSO-*d*₆) δ 10.29 (s, 1H), 7.71 (d, $J = 7.8$ Hz, 1H), 7.30 (t, $J = 7.6$ Hz, 1H), 7.21 (dd, $J = 7.6$, 1.5 Hz, 1H), 7.18 (dd, $J = 7.5$, 1.5 Hz, 1H), 7.00–6.93 (m, 2H), 6.92 (d, $J = 8.2$ Hz, 1H), 6.86 (d, $J = 2.1$ Hz, 1H), 6.81 (dd, $J = 8.2$, 2.1 Hz, 1H), 4.28 (s, 4H), 2.07 (s, 3H). ESI-MS: $m/z = 347$ [M+H]⁺.

4.1.64. 3'-(2,3-dihydrobenzo[b][1,4]dioxin-6-yl)-4-(((2-hydroxyethyl)amino)methyl)-2'-methyl-[1,1'-biphenyl]-3-ol **36**

General procedure D. Yield: 76%; ¹H NMR (500 MHz, Chloroform-*d*) δ 7.24–7.17 (m, 2H), 7.20–7.14 (m, 1H), 7.05 (d, $J = 7.6$ Hz, 1H), 6.90 (d, $J = 8.2$ Hz, 1H), 6.87 (d, $J = 2.0$ Hz, 2H), 6.82 (dd, $J = 8.2$, 2.1 Hz, 1H), 6.77 (dd, $J = 7.6$, 1.4 Hz, 1H), 4.30 (s, 4H), 4.11 (s, 2H), 3.84 (t, $J = 4.9$ Hz, 2H), 3.71 (s, 1H), 2.92 (t, $J = 4.9$ Hz, 2H), 2.12 (s, 3H). ESI-MS: $m/z = 391$ [M+H]⁺.

4.1.65. 7-(3-(2,3-dihydrobenzo[b][1,4]dioxin-6-yl)-2-methylphenyl)-3-(2-hydroxyethyl)-3,4-dihydro-2H-benzo[e][1,3]oxazin-2-one **B13**

To a solution of **36** (100 mg, 0.256 mmol) and pyridine in DCM (5 mL) and TBSOTf (102 mg, 0.384 mmol) was added, and the reaction was allowed to stir at room temperature. After TLC monitoring, the reaction mixture was extracted with DCM and saturated NH₄Cl solution, dried over sodium sulfate, and concentrated under vacuum. To the solution of the above residues, Et₃N (39 mg, 0.384 mmol) and DCM (5 mL) were added, and the reaction was allowed to stir at room temperature with the addition of

Triphosgene (114 mg, 0.384 mmol). After TLC monitoring, 12 N HCl (2 mL) was added, and the reaction mixture was allowed to stir at room temperature for 30 min. After TLC monitoring, the reaction mixture was purified by column chromatography using silica gel to yield **B14** (14 mg). Yield: 13%; ¹H NMR (500 MHz, DMSO-*d*₆) δ 7.29 (dd, $J = 16.7$, 7.8 Hz, 2H), 7.19–7.12 (m, 3H), 7.02 (d, $J = 1.6$ Hz, 1H), 6.91 (d, $J = 8.2$ Hz, 1H), 6.85 (d, $J = 2.0$ Hz, 1H), 6.81 (dd, $J = 8.2$, 2.1 Hz, 1H), 5.31 (t, $J = 4.9$ Hz, 1H), 4.95 (t, $J = 5.5$ Hz, 1H), 4.65 (s, 2H), 4.27 (s, 4H), 3.64 (q, $J = 5.6$ Hz, 2H), 2.07 (s, 3H). ESI-MS: $m/z = 418$ [M+H]⁺. HRMS (ESI) for C₂₅H₂₃NO₅ [M+H]⁺, calcd: 418.1654, found: 418.1642.

4.1.66. tert-butyl ((3'-(2,3-dihydrobenzo[b][1,4]dioxin-6-yl)-3-hydroxy-2'-methyl-[1,1'-biphenyl]-4-yl)methyl)glycinate **37**

General procedure D. Yield: 85%; ¹H NMR (500 MHz, Chloroform-*d*) δ 7.24–7.21 (m, 1H), 7.21–7.17 (m, 2H), 7.03 (d, $J = 7.6$ Hz, 1H), 6.90 (d, $J = 8.2$ Hz, 1H), 6.88 (t, $J = 1.7$ Hz, 2H), 6.82 (dd, $J = 8.2$, 2.1 Hz, 1H), 6.78 (dd, $J = 7.6$, 1.7 Hz, 1H), 4.30 (s, 4H), 4.06 (s, 2H), 3.41 (s, 2H), 2.14 (s, 3H), 1.49 (s, 9H). ESI-MS: $m/z = 462$ [M+H]⁺.

4.1.67. 2-(7-(3-(2,3-dihydrobenzo[b][1,4]dioxin-6-yl)-2-methylphenyl)-2-oxo-2H-benzo[e][1,3]oxazin-3(4H)-yl)acetic acid **B14**

To a solution of **37** (100 mg, 0.217 mmol) and Et₃N (33 mg, 0.325 mmol) in DCM (5 mL) and triphosgene (97 mg, 0.325 mmol) was added, and the reaction was allowed to stir at room temperature. After TLC monitoring, the reaction mixture was concentrated, saturated NaHCO₃ solution was added, and extracted with ethyl acetate. Combined organic layers were dried over sodium sulfate, and concentrated under vacuum. Then CF₃COOH (2.5 mL) and DCM (5 mL) were added, and the reaction was allowed to stir overnight at room temperature. After TLC monitoring, the reaction mixture was purified by column chromatography using silica gel to yield **B15** (12 mg). Yield: 13%; ¹H NMR (500 MHz, DMSO-*d*₆) δ 7.31 (d, $J = 8.1$ Hz, 1H), 7.28 (d, $J = 7.6$ Hz, 1H), 7.20–7.13 (m, 3H), 7.04 (d, $J = 1.7$ Hz, 1H), 6.92 (d, $J = 8.2$ Hz, 1H), 6.86 (d, $J = 2.1$ Hz, 1H), 6.81 (dd, $J = 8.2$, 2.1 Hz, 1H), 4.61 (s, 2H), 4.28 (s, 4H), 3.87 (s, 2H), 2.07 (s, 3H). ESI-MS: $m/z = 432$ [M+H]⁺. HRMS (ESI) for C₂₅H₂₁NO₆ [M+H]⁺, calcd: 432.1447, found: 432.1430.

4.1.68. tert-butyl (2-amino-4-bromobenzyl)glycinate **39**

General procedure D. Yield: 69%; ¹H NMR (500 MHz, Chloroform-*d*) δ 6.85 (d, $J = 7.9$ Hz, 1H), 6.79 (d, $J = 1.9$ Hz, 1H), 6.76 (dd, $J = 7.9$, 1.9 Hz, 1H), 3.73 (s, 2H), 3.27 (s, 2H), 1.47 (s, 9H). ESI-MS: $m/z = 317$.

4.1.69. 8-bromo-1,3,4,5-tetrahydro-2H-benzo[e][1,4]diazepin-2-one **40**

To a solution of **39** (100 mg, mmol) in DCM (5 mL), CF₃COOH (2.5 mL) was added and the reaction was stirred at room temperature. After TLC monitoring, DCM and CF₃COOH were evaporated under vacuum. Then toluene (5 mL) was added, and the reaction was allowed to reflux. After TLC monitoring, the reaction mixture was purified by column chromatography using silica gel to yield **40** (52 mg). Yield: 68%; ¹H NMR (500 MHz, Chloroform-*d*) δ 7.19 (dd, $J = 8.1$, 1.9 Hz, 1H), 7.11 (d, $J = 1.9$ Hz, 1H), 7.05 (d, $J = 8.1$ Hz, 1H), 3.98 (s, 2H), 3.71 (s, 2H). ESI-MS: $m/z = 243$.

4.1.70. 8-(3-(2,3-dihydrobenzo[b][1,4]dioxin-6-yl)-2-methylphenyl)-4-(2-hydroxyethyl)-1,3,4,5-tetrahydro-2H-benzo[e][1,4]diazepin-2-one **B15**

A solution of **40** (50 mg, 0.2 mmol), **31** (73 mg, 0.2 mmol), Pd(dppf)Cl₂·DCM (17 mg, 0.02 mmol) and KOAc (61 mg, 0.62 mmol) in 1,4-dioxane (5 mL) was refluxed for 16 h under a nitrogen atmosphere. After TLC monitoring, the reaction mixture was

concentrated, saturated NaHCO₃ solution was added, and extracted with ethyl acetate. Combined organic layers were dried over sodium sulfate, and concentrated under vacuum. To the residue in DCM (5 mL) and 2-bromoethanol (39 mg, 0.62 mmol) and Et₃N (63 mg, 0.62 mmol) were added, and the reaction mixture was stirred at room temperature. After TLC monitoring, the crude product was purified by column chromatography using silica gel to yield **B16** (12 mg). Yield: 13%; ¹H NMR (500 MHz, Chloroform-*d*) δ 7.30 (d, *J* = 7.9 Hz, 1H), 7.24 (d, *J* = 1.9 Hz, 1H), 7.18–7.16 (m, 1H), 7.14 (dd, *J* = 7.7, 1.7 Hz, 1H), 7.06 (d, *J* = 7.9 Hz, 2H), 6.92 (d, *J* = 8.2 Hz, 1H), 6.87 (d, *J* = 2.0 Hz, 1H), 6.83–6.80 (m, 1H), 4.31 (s, 4H), 3.99 (s, 2H), 3.94 (s, 2H), 3.85–3.80 (m, 2H), 2.92–2.89 (m, 2H), 2.12 (s, 3H). HRMS (ESI) for C₂₆H₂₆N₂O₄ [M+H]⁺, calcd: 431.1971, found: 431.1952.

4.1.71. 2-(7-(3-(2,3-dihydrobenzo[*b*] [1,4]dioxin-6-yl)-2-methylphenyl)-1,3,4,5-tetrahydro-2H-benzo[*c*]azepin-2-yl)ethan-1-ol **B16**

Synthesized following a protocol similar to compound **B16**, with the replacement of **40** with **41** to yield **B17** (10 mg). Yield: 11%; ¹H NMR (500 MHz, DMSO-*d*₆) δ 7.48 (d, *J* = 1.8 Hz, 1H), 7.44–7.35 (m, 2H), 7.29 (d, *J* = 7.7 Hz, 1H), 7.19 (ddd, *J* = 7.4, 4.3, 1.4 Hz, 2H), 6.93 (d, *J* = 8.2 Hz, 1H), 6.84 (d, *J* = 2.0 Hz, 1H), 6.80 (dd, *J* = 8.2, 2.1 Hz, 1H), 4.28 (s, 4H), 3.91 (s, 2H), 3.82 (s, 2H), 3.52–3.46 (m, 2H), 3.06 (s, 2H), 2.08 (d, *J* = 2.4 Hz, 5H), 1.23 (s, 2H). ESI-MS: *m/z* = 416 [M+H]⁺.

4.1.72. 4-(4,4,5,5-tetramethyl-1,3,2-dioxaborolan-2-yl)-1H-indole **42**

General procedure B. Yield: 89%; ¹H NMR (500 MHz, DMSO-*d*₆) δ 11.09 (s, 1H), 7.52 (dt, *J* = 8.1, 1.0 Hz, 1H), 7.40 (dd, *J* = 7.0, 1.1 Hz, 1H), 7.37 (t, *J* = 2.7 Hz, 1H), 7.08 (dd, *J* = 8.1, 7.0 Hz, 1H), 6.76 (ddd, *J* = 3.0, 2.0, 0.9 Hz, 1H), 1.33 (s, 12H). ESI-MS: *m/z* = 244 [M+H]⁺.

4.1.73. 1H,1'H-4,4'-biindole **43**

General procedure G. Yield: 66%; ¹H NMR (500 MHz, DMSO-*d*₆) δ 11.21 (s, 2H), 7.44 (pd, *J* = 3.6, 1.0 Hz, 2H), 7.36 (t, *J* = 2.8 Hz, 2H), 7.21 (dd, *J* = 4.7, 0.8 Hz, 4H), 6.38 (ddd, *J* = 3.0, 1.9, 0.9 Hz, 2H). ESI-MS: *m/z* = 233 [M+H]⁺.

4.1.74. 1H,1'H-[4,4'-biindole]-1,1'-diylbis((4-(bromomethyl)phenyl)methanone) **44**

General procedure F. Yield: 73%; ¹H NMR (500 MHz, DMSO-*d*₆) δ 8.38 (d, *J* = 8.2 Hz, 2H), 7.79 (d, *J* = 8.2 Hz, 4H), 7.67 (d, *J* = 8.3 Hz, 4H), 7.54 (t, *J* = 7.8 Hz, 2H), 7.45–7.42 (m, 4H), 6.51 (d, *J* = 3.9 Hz, 2H), 4.82 (s, 4H). ESI-MS: *m/z* = 628.

4.1.75. 1H,1'H-[4,4'-biindole]-1,1'-diylbis((4-(((2-hydroxyethyl)amino)methyl)phenyl)methanone) **C1**

General procedure E. Yield: 35%; HPLC: t_R 12.442 min, purity > 95%. ¹H NMR (500 MHz, DMSO-*d*₆) δ 8.36 (d, *J* = 8.5 Hz, 2H), 7.75 (d, *J* = 7.8 Hz, 4H), 7.56 (d, *J* = 8.1 Hz, 4H), 7.52 (s, 2H), 7.49–7.43 (m, 4H), 7.40 (s, 2H), 6.53 (s, 2H), 3.83 (s, 4H), 3.49 (s, 4H), 2.89 (s, 4H). ESI-MS: *m/z* = 587 [M+H]⁺; *m/z* = 294 [M/2 + H]⁺.

4.1.76. [4,4'-biindoline]-1,1'-diylbis((4-(((2-hydroxyethyl)amino)methyl)phenyl)methanone) **C2**

To flask containing **C1** (20 mg, 0.034 mmol) was added HAc (5 mL) in 0 °C. NaBH₃CN (21 mg, 0.34 mmol) was added and then stirred at room temperature for 2 h. After TLC monitoring, the reaction mixture was alkalinized with 50% NaOH, extracted with DCM, dried over sodium sulfate, and concentrated under vacuum. The crude product was then purified by column chromatography using silica gel to yield **C2** (12 mg). Yield: 60%; ¹H NMR (500 MHz, DMSO-*d*₆) δ 7.43 (d, *J* = 7.8 Hz, 4H), 7.40–7.37 (m, 1H), 7.33 (d, *J* = 7.6 Hz, 4H), 7.28 (d, *J* = 7.7 Hz, 1H), 7.16 (s, 2H), 6.88 (d, *J* = 7.7 Hz,

2H), 3.88 (t, *J* = 8.2 Hz, 4H), 3.66 (s, 4H), 2.82 (t, *J* = 8.4 Hz, 4H), 2.78 (s, 2H), 2.62 (s, 2H), 2.46 (t, *J* = 5.9 Hz, 4H). ESI-MS: *m/z* = 591 [M+H]⁺; *m/z* = 296 [M/2 + H]⁺

4.1.77. 2-methyl-3-(4,4,5,5-tetramethyl-1,3,2-dioxaborolan-2-yl)phenol **45**

General procedure B. Yield: 99%; ¹H NMR (500 MHz, DMSO-*d*₆) δ 9.19 (s, 1H), 7.07 (dd, *J* = 7.3, 1.4 Hz, 1H), 6.96 (t, *J* = 7.6 Hz, 1H), 6.87 (dd, *J* = 7.9, 1.5 Hz, 1H), 2.29 (s, 3H), 1.28 (s, 12H); ¹³C NMR (126 MHz, DMSO) δ 155.13, 130.04, 126.11, 125.66, 117.17, 83.17, 40.11, 40.02, 39.95, 39.86, 39.78, 39.69, 39.61, 39.52, 39.35, 39.19, 39.02, 24.68, 14.66. ESI-MS: *m/z* = 235 [M+H]⁺.

4.1.78. 2,2'-dimethyl-[1,1'-biphenyl]-3,3'-diol **46**

General procedure G. Yield: 62%; ¹H NMR (500 MHz, DMSO-*d*₆) δ 9.33 (s, 2H), 6.99 (t, *J* = 7.8 Hz, 2H), 6.78 (dd, *J* = 8.0, 1.2 Hz, 2H), 6.48 (dd, *J* = 7.5, 1.3 Hz, 2H), 1.79 (s, 6H); ¹³C NMR (126 MHz, DMSO) δ 155.30, 142.73, 125.76, 121.87, 119.81, 113.24, 12.76. ESI-MS: *m/z* = 215 [M+H]⁺.

4.1.79. 2,2'-(2,2'-dimethyl-[1,1'-biphenyl]-3,3'-diyl)bis(4,4,5,5-tetramethyl-1,3,2-dioxaborolane) **47**

To a solution of **46** (352 mg, 1.64 mmol) in DCM (10 mL), pyridine (390 mg, 4.929 mmol) and trifluoromethanesulfonic anhydride (1.112 g, 3.9 mmol) were added and the reaction was allowed to stir overnight at room temperature. After TLC monitoring, to the reaction mixture hydrochloric acid was added, and extracted with DCM. Combined organic layers were washed with saturated NaHCO₃ solution and brine, dried over sodium sulfate, and concentrated under vacuum. This was taken as such to the next step without further purification. A solution of phenyl trifluoromethanesulfonate (700 mg, 1.6 mmol), Bis(pinacolato)diboron (900 mg, 3.5 mmol), Pd (dppf)Cl₂ (250 mg, 0.3 mmol) and KOAc (600 mg, 5.8 mmol) in dioxane (10 mL) was refluxed under a nitrogen atmosphere. The crude product was then purified by column chromatography using silica gel to yield **47** (450 mg). Yield: 70%; ¹H NMR (500 MHz, DMSO-*d*₆) δ 7.64 (dd, *J* = 7.5, 1.6 Hz, 2H), 7.22 (t, *J* = 7.4 Hz, 2H), 7.10 (dd, *J* = 7.5, 1.6 Hz, 2H), 2.11 (s, 6H), 1.31 (s, 24H); ¹³C NMR (126 MHz, DMSO) δ 170.35, 141.76, 141.10, 134.64, 131.84, 124.89, 83.42, 24.65, 14.10. ESI-MS: *m/z* = 435 [M+H]⁺.

4.1.80. 2',2''-dimethyl-[1,1':3',1'':3'',1'''-quaterphenyl]-4,4'''-dicarbaldehyde **48a**

General procedure G. Yield: 67%; ¹H NMR (500 MHz, Chloroform-*d*) δ 10.08 (s, 2H), 7.96 (d, *J* = 8.2 Hz, 4H), 7.55 (d, *J* = 8.2 Hz, 4H), 7.34 (t, *J* = 7.5 Hz, 2H), 7.26 (s, 1H), 7.23 (td, *J* = 7.5, 7.0, 1.5 Hz, 3H), 1.99 (s, 6H). ESI-MS: *m/z* = 391 [M+H]⁺.

4.1.81. 6,6''-(2,2'-dimethyl-[1,1'-biphenyl]-3,3'-diyl)dinicotinaldehyde **48b**

General procedure G. Yield: 72%; ¹H NMR (500 MHz, Chloroform-*d*) δ 10.17 (s, 2H), 9.17 (dd, *J* = 2.3, 0.8 Hz, 2H), 8.26 (dd, *J* = 8.1, 2.2 Hz, 2H), 7.64 (dt, *J* = 8.1, 0.7 Hz, 2H), 7.43 (dd, *J* = 7.7, 1.5 Hz, 2H), 7.37 (t, *J* = 7.6 Hz, 2H), 7.29–7.26 (m, 2H), 2.08 (s, 6H). ¹³C NMR (126 MHz, CDCl₃) δ 190.66, 165.81, 151.94, 142.89, 140.21, 136.09, 133.97, 130.62, 129.68, 129.08, 125.96, 125.01, 17.88. ESI-MS: *m/z* = 393 [M+H]⁺.

4.1.82. 3,3'''-dimethoxy-2',2''-dimethyl-[1,1':3',1'':3'',1'''-quaterphenyl]-4,4'''-dicarbaldehyde **48c**

General procedure G. Yield: 83%; ¹H NMR (500 MHz, DMSO-*d*₆) δ 10.39 (s, 2H), 7.76 (d, *J* = 7.9 Hz, 2H), 7.38 (t, *J* = 7.5 Hz, 2H), 7.31 (dd, *J* = 7.7, 1.5 Hz, 2H), 7.22 (td, *J* = 4.3, 3.8, 1.5 Hz, 4H), 7.12–7.08 (m, 2H), 3.97 (s, 6H), 1.97 (s, 6H). ¹³C NMR (126 MHz, DMSO) δ 188.82, 161.35, 149.85, 142.23, 141.17, 132.50, 129.10, 128.51, 127.65,

125.78, 122.82, 121.85, 113.58, 56.17, 17.88. ESI-MS: $m/z = 451$ [M+H]⁺.

4.1.83. 2,2'-(((2,2''-dimethyl-[1,1':3',1'':3''',1'''-quaterphenyl]-4,4''''-diyl)bis(methylene))bis(azanediy))bis(ethan-1-ol) **C3**

General procedure D. Yield: 13%; ¹H NMR (500 MHz, DMSO-*d*₆) δ 7.42 (d, *J* = 8.1 Hz, 4H), 7.35–7.30 (m, 6H), 7.21 (dd, *J* = 7.6, 1.5 Hz, 2H), 7.14 (dd, *J* = 7.5, 1.5 Hz, 2H), 4.57 (s, 2H), 3.80 (s, 4H), 3.51 (d, *J* = 5.1 Hz, 4H), 3.17 (d, *J* = 5.0 Hz, 2H), 2.67–2.63 (m, 4H), 1.92 (s, 6H). ESI-MS: $m/z = 481$ [M+H]⁺.

4.1.84. 2,2'-(((2,2''-dimethyl-[1,1'-biphenyl]-3,3'-diyl)bis(pyridine-6,3-diy))bis(methylene))bis(azanediy))bis(ethan-1-ol) **C4**

General procedure D. Yield: 15%; ¹H NMR (500 MHz, DMSO-*d*₆) δ 8.62–8.54 (m, 2H), 7.85–7.76 (m, 2H), 7.50 (d, *J* = 8.0 Hz, 2H), 7.38–7.34 (m, 4H), 7.21–7.16 (m, 2H), 3.78 (s, 4H), 3.50 (d, *J* = 6.0 Hz, 2H), 3.17 (s, 2H), 2.65–2.58 (m, 2H), 2.19 (s, 2H), 1.99–1.97 (m, 6H). ESI-MS: $m/z = 483$ [M+H]⁺.

4.1.85. 2,2'-(((3,3'''-dimethoxy-2',2''-dimethyl-[1,1':3',1'':3''',1'''-quaterphenyl]-4,4''''-diyl)bis(methylene))bis(azanediy))bis(ethan-1-ol) **C5**

General procedure D. Yield: 15%; HPLC: *t*_R 13.291 min, purity 98.48%. ESI-MS: $m/z = 541$ [M+H]⁺.

4.1.86. 2-(((4'''-(hydroxymethyl)-3,3'''-dimethoxy-2',2''-dimethyl-[1,1':3',1'':3''',1'''-quaterphenyl]-4-yl)methyl)amino)propane-1,3-diol **C6**

General procedure D. Yield: 46%; ¹H NMR (500 MHz, DMSO-*d*₆) δ 7.44 (dd, *J* = 21.5, 7.6 Hz, 2H), 7.35–7.29 (m, 2H), 7.24 (d, *J* = 7.5 Hz, 2H), 7.15 (t, *J* = 8.0 Hz, 2H), 7.01–6.90 (m, 4H), 5.05 (t, *J* = 5.6 Hz, 1H), 4.52 (d, *J* = 5.6 Hz, 2H), 3.85 (s, 3H), 3.80 (s, 3H), 3.52 (d, *J* = 23.9 Hz, 6H), 3.16 (d, *J* = 5.1 Hz, 2H), 2.54 (s, 1H), 1.95 (d, *J* = 2.7 Hz, 6H). ESI-MS: $m/z = 528$ [M+H]⁺. HRMS (ESI) for C₃₃H₃₇NO₅ [M+H]⁺, calcd: 528.2750, found: 528.2770.

4.1.87. 2,2'-(((3,3'''-dimethoxy-2',2''-dimethyl-[1,1':3',1'':3''',1'''-quaterphenyl]-4,4''''-diyl)bis(methylene))bis(azanediy))bis(propane-1,3-diol) **C7**

General procedure D. Yield: 31%; ¹H NMR (500 MHz, DMSO-*d*₆) δ 7.52 (d, *J* = 7.7 Hz, 2H), 7.34 (t, *J* = 7.6 Hz, 2H), 7.25 (dd, *J* = 7.7, 1.5 Hz, 2H), 7.17 (dd, *J* = 7.5, 1.5 Hz, 2H), 7.03 (s, 2H), 6.98 (d, *J* = 7.6 Hz, 2H), 5.21 (s, 4H), 4.14 (q, *J* = 5.3 Hz, 4H), 3.87 (s, 6H), 3.64 (s, 8H), 2.54–2.52 (m, 2H), 1.96 (s, 6H). ESI-MS: $m/z = 601$ [M+H]⁺.

4.1.88. *N,N'*-(((3,3'''-dimethoxy-2',2''-dimethyl-[1,1':3',1'':3''',1'''-quaterphenyl]-4,4''''-diyl)bis(methylene))bis(tetrahydro-2H-pyran-4-amine) **C8**

General procedure D. Yield: 50%; ¹H NMR (500 MHz, DMSO-*d*₆) δ 7.53 (d, *J* = 7.9 Hz, 2H), 7.34 (t, *J* = 7.5 Hz, 2H), 7.25 (d, *J* = 7.4 Hz, 2H), 7.17 (d, *J* = 7.5 Hz, 2H), 7.01 (s, 2H), 6.97 (d, *J* = 7.6 Hz, 2H), 4.14 (s, 2H), 3.99 (s, 4H), 3.90 (d, *J* = 10.0 Hz, 6H), 3.86 (s, 8H), 2.56–2.53 (m, 2H), 1.96 (s, 6H), 1.83 (d, *J* = 22.5 Hz, 4H), 1.53 (td, *J* = 12.1, 4.7 Hz, 4H). ESI-MS: $m/z = 621$ [M+H]⁺. HRMS (ESI) for C₄₀H₄₈N₂O₄ [M+H]⁺, calcd: 621.3692, found: 621.3647.

4.1.89. 2,2'-(((3,3'''-dimethoxy-2',2''-dimethyl-[1,1':3',1'':3''',1'''-quaterphenyl]-4,4''''-diyl)bis(methylene))bis(azanediy))bis(cyclopentan-1-ol) **C9**

General procedure D. Yield: 47%; ¹H NMR (500 MHz, DMSO-*d*₆) δ 7.53 (s, 2H), 7.34 (t, *J* = 7.6 Hz, 2H), 7.25 (dd, *J* = 7.7, 1.5 Hz, 2H), 7.19–7.15 (m, 2H), 7.03 (s, 2H), 6.98 (d, *J* = 7.6 Hz, 2H), 4.24–4.09 (m, 4H), 4.03 (d, *J* = 10.5 Hz, 2H), 3.87 (s, 6H), 2.55–2.52 (m, 2H), 1.96 (s, 6H), 1.64 (s, 6H), 1.48 (dd, *J* = 13.1, 6.9 Hz, 4H). ESI-MS: $m/z = 621$ [M+H]⁺. HRMS (ESI) for C₄₀H₄₈N₂O₄ [M+H]⁺, calcd: 621.3692, found: 621.3671.

found: 621.3671.

4.1.90. 5,5'-((((3,3'''-dimethoxy-2',2''-dimethyl-[1,1':3',1'':3''',1'''-quaterphenyl]-4,4''''-diyl)bis(methylene))bis(azanediy))bis(methylene))bis(pyrrrolidin-2-one) **C10**

General procedure D. Yield: 34%; ¹H NMR (500 MHz, DMSO-*d*₆) δ 7.72 (s, 2H), 7.40 (d, *J* = 7.6 Hz, 2H), 7.32 (t, *J* = 7.6 Hz, 2H), 7.24 (d, *J* = 7.5 Hz, 2H), 7.15 (d, *J* = 7.4 Hz, 2H), 6.96–6.90 (m, 4H), 3.82 (s, 6H), 3.78–3.73 (m, 4H), 3.66 (d, *J* = 7.4 Hz, 2H), 2.59 (d, *J* = 6.0 Hz, 4H), 1.90 (s, 6H), 1.75 (s, 2H), 1.71–1.67 (m, 2H), 1.67–1.59 (m, 2H). ESI-MS: $m/z = 647$ [M+H]⁺.

4.1.91. (3,3'''-dimethoxy-2',2''-dimethyl-[1,1':3',1'':3''',1'''-quaterphenyl]-4,4''''-diyl)dimethanol **C11**

General procedure D. Yield: 64%; ¹H NMR (500 MHz, DMSO-*d*₆) δ 7.42 (d, *J* = 7.5 Hz, 2H), 7.32 (t, *J* = 7.6 Hz, 2H), 7.24 (dd, *J* = 7.7, 1.5 Hz, 2H), 7.15 (dd, *J* = 7.5, 1.5 Hz, 2H), 6.96–6.91 (m, 4H), 5.03 (t, *J* = 5.7 Hz, 2H), 4.53 (d, *J* = 5.7 Hz, 4H), 3.81 (s, 6H), 1.95 (s, 6H). ESI-MS: $m/z = 455$ [M+H]⁺.

4.1.92. 1-(((4'''-(hydroxymethyl)-3,3'''-dimethoxy-2',2''-dimethyl-[1,1':3',1'':3''',1'''-quaterphenyl]-4-yl)methyl)piperidine-2-carboxylic acid) **C12**

General procedure D. Yield: 21%; ¹H NMR (500 MHz, DMSO-*d*₆) δ 7.48 (d, *J* = 7.6 Hz, 1H), 7.42 (d, *J* = 7.6 Hz, 1H), 7.32 (dt, *J* = 7.7, 3.8 Hz, 2H), 7.25 (t, *J* = 8.0 Hz, 2H), 7.15 (dd, *J* = 7.3, 4.2 Hz, 2H), 6.98–6.90 (m, 4H), 4.53 (s, 2H), 3.82 (s, 3H), 3.80 (s, 3H), 3.65 (s, 2H), 1.95 (d, *J* = 5.5 Hz, 6H), 1.90 (s, 3H), 1.85 (q, *J* = 4.5, 3.5 Hz, 3H), 1.75 (s, 4H). ESI-MS: $m/z = 566$ [M+H]⁺. HRMS (ESI) for C₃₆H₃₉NO₅ [M+H]⁺, calcd: 566.2906, found: 566.2907.

4.1.93. 1,1'-(((3,3'''-dimethoxy-2',2''-dimethyl-[1,1':3',1'':3''',1'''-quaterphenyl]-4,4''''-diyl)bis(methylene))bis(azetidone-3-carboxylic acid) **C13**

General procedure D. Yield: 27%; ¹H NMR (500 MHz, DMSO-*d*₆) δ 10.07 (s, 2H), 7.45 (d, *J* = 7.7 Hz, 2H), 7.35 (t, *J* = 7.6 Hz, 2H), 7.26 (dd, *J* = 7.8, 1.5 Hz, 2H), 7.18 (dd, *J* = 7.5, 1.4 Hz, 2H), 7.09 (d, *J* = 1.7 Hz, 2H), 7.02 (dd, *J* = 7.6, 1.5 Hz, 2H), 4.50–4.35 (m, 5H), 4.24 (d, *J* = 9.6 Hz, 10H), 1.95 (s, 6H). ¹³C NMR (126 MHz, DMSO) δ 157.87, 142.74, 141.92, 132.97, 129.16, 126.12, 121.99, 112.75, 56.31, 40.48, 40.40, 40.31, 40.23, 40.14, 40.06, 39.98, 39.90, 39.81, 39.64, 39.55, 39.48, 32.58, 18.35. ESI-MS: $m/z = 621$ [M+H]⁺. HRMS (ESI) for C₃₈H₄₀N₂O₆ [M+H]⁺, calcd: 621.2965, found: 621.2948.

4.1.94. 2,2'-(((3,3'''-dimethoxy-2',2''-dimethyl-[1,1':3',1'':3''',1'''-quaterphenyl]-4,4''''-diyl)bis(methylene))bis(azanediy))bis(3-hydroxypropanoic acid) **C14**

General procedure D. Yield: 31%; HPLC: *t*_R 15.956 min, purity 96.30%. ¹H NMR (500 MHz, DMSO-*d*₆) δ 9.14 (s, 2H), 7.48 (d, *J* = 7.7 Hz, 2H), 7.35 (t, *J* = 7.6 Hz, 2H), 7.26 (dd, *J* = 7.8, 1.4 Hz, 2H), 7.18 (dd, *J* = 7.5, 1.4 Hz, 2H), 7.06 (d, *J* = 1.5 Hz, 2H), 7.01 (dd, *J* = 7.6, 1.5 Hz, 2H), 4.29 (d, *J* = 13.3 Hz, 2H), 4.21 (d, *J* = 13.3 Hz, 2H), 3.95–3.83 (m, 14H), 1.96 (s, 6H). ¹³C NMR (126 MHz, DMSO) δ 173.03, 157.90, 144.94, 142.73, 142.02, 132.97, 131.82, 129.13, 126.12, 121.79, 118.50, 112.58, 99.99, 66.50, 56.32, 49.19, 45.85, 40.56, 40.47, 40.39, 40.30, 40.22, 40.13, 40.06, 39.97, 39.89, 39.80, 39.63, 39.53, 39.46, 18.36. ESI-MS: $m/z = 629$ [M+H]⁺. HRMS (ESI) for C₃₆H₄₀N₂O₈ [M+H]⁺, calcd: 629.2863, found: 629.2847.

4.1.95. 3,3'-(((3,3'''-dimethoxy-2',2''-dimethyl-[1,1':3',1'':3''',1'''-quaterphenyl]-4,4''''-diyl)bis(methylene))bis(azanediy))bis(2-hydroxypropanoic acid) **C15**

General procedure D. Yield: 27%; ¹H NMR (500 MHz, DMSO-*d*₆) δ 8.81 (s, 2H), 7.48 (d, *J* = 7.7 Hz, 2H), 7.36 (t, *J* = 7.6 Hz, 2H), 7.27 (d, *J* = 7.4 Hz, 2H), 7.19 (d, *J* = 7.4 Hz, 2H), 7.09 (s, 2H), 7.02 (d, *J* = 7.5 Hz,

2H), 6.35–6.21 (m, 2H), 4.40 (dd, $J = 9.6, 3.4$ Hz, 2H), 4.22 (q, $J = 13.3$ Hz, 4H), 3.89 (s, 6H), 3.25 (d, $J = 12.7$ Hz, 4H), 3.08 (t, $J = 11.1$ Hz, 2H), 1.96 (s, 6H). ^{13}C NMR (126 MHz, DMSO) δ 169.17, 158.05, 144.88, 142.75, 142.05, 132.97, 132.14, 129.10, 126.10, 121.81, 118.51, 112.49, 60.73, 59.44, 56.20, 44.50, 40.57, 40.48, 40.41, 40.31, 40.24, 40.15, 40.07, 39.98, 39.82, 39.65, 39.48, 18.36. ESI-MS: $m/z = 629$ $[\text{M}+\text{H}]^+$. HRMS (ESI) for $\text{C}_{36}\text{H}_{40}\text{N}_2\text{O}_8$ $[\text{M}+\text{H}]^+$, calcd: 629.2863, found: 629.2841.

4.2. Homogeneous time resolved fluorescence (HTRF assay)

The PD-1/PD-L1 Binding Assay Kits were bought from CISBIO (Cat#64ICP01PEH). The compounds were sequentially diluted following a concentration gradient. In a 96-well plate, 2 μL of the target compounds dilution was mixed with 4 μL of Tag 1-PD-L1 protein, and 4 μL of Tag 2- PD-1 protein, successively. The mixtures were in-cubated for 15 min at room temperature (RT). Then the mixture of 10 μL anti-Tag1-Eu3+ and anti-Tag2-XL665 were added, and the plate was sealed to incubate for 2 h at RT in the dark. Finally, the fluorescence signal was detected at 665 nm and 620 nm. The IC_{50} values were calculated using Graphpad 8.0.2 software.

4.3. Cell-based PD-1/PD-L1 immune checkpoint blockade bioassay

Hep3B-OS8-hPDL1 cells were cultured in 1640 medium supplemented with 10% fetal bovine serum, 1% penicillin and streptomycin, in which 100 $\mu\text{g}/\text{mL}$ G418 and Hygromycin B were also added and were seeded into 96-well flat bottom plate (1.25×10^4 cells/100 $\mu\text{L}/\text{well}$). The medium was removed from the wells, and compound or antibody dilutions (prepared in DMSO and further diluted by different folds in fresh assay buffer (RPMI 1640 containing 10% FBS) to a final DMSO concentration below 0.3%.) were added. Jurkat-NFAT-PD-1 cells were then seeded into 96-well flat bottom plate (1.25×10^4 cells/50 $\mu\text{L}/\text{well}$) and allowed to incubate at 37 $^\circ\text{C}$ and 5% CO_2 for 6 h. Equilibrate cultured cells at room temperature for 5–10 min. Add equal volume (100 $\mu\text{L}/\text{well}$) of ONE-GloTM Luciferase Assay System to each well, wait at least 3 min to allow complete cell lysis and measure in a luminometer. The data and EC_{50} values were calculated using Graphpad 8.0.2 software.

4.4. Cytotoxicity assay

The cytotoxicity was detected with the CCK8 assay. The HPDE6-C7, HL7702 cells and PBMC were cultured in 96-well plates for 24 h. The compounds were sequentially diluted and was mixed with 0.1% DMSO in total 100 μL of medium. Then the solutions were added and co-cultured for 2 days. The 10 μL solution of CCK8 was added and co-cultured for 4 h. Then the fluorescence signal at 450 nm was tested by a microplate reader and the figure was graphed using Graphpad 8.0.2 software.

4.5. Determination of IFN- γ secretion

The 293T-OS8-hPDL1 cells were treated with Mitomycin C for 1.5 h and washed with PBS thrice. The cells (50,000 cells/well) were added to a 96-well plate. After 2 h, the cells were treated with different concentrations of the respective compounds (100 μL hPD-L1 and 1 μL compounds). After another 4 h, the $\text{CD}3^+$ T cells were extracted, counted, and added to the 96-well plates. Then, the compounds were added and co-cultured at 37 $^\circ\text{C}$. After 36 h, the supernatants were collected to estimate the levels of IFN- γ . The result was treated with Graphpad 8.0.2 software.

4.6. hERG inhibition assay

Currents were recorded from HEK-293 cells, using the whole-cell patch-clamp technique. The cells were transferred to a perfusion chamber, and the perfusion was performed with extracellular fluid (mM): K aspartate, 130; MgCl_2 , 5; EGTA, 5; HEPES, 10; Tris-ATP, 4; pH 7.2. Electrodes were pulled using a dualstage glass micropipette puller (Narishige PC-10, Japan). Current traces of hERG channels were elicited by applying a pulse from -80 to $+40$ mV for 4 s followed by a step to -40 mV for 2 s. The procedure was repeated every 20 s. After the maximum current was stabilized, the tested compounds (10 μM) were perfused. The inhibition rate was calculated when the current was stable.

4.7. Molecular docking and dynamic simulation

The crystal structure of PD-L1 (PDB ID: 6RPG) was obtained from <http://www.rcsb.org/> and treated using Schrödinger Procedures such as residual repair, hydrogen optimization, water removal, and energy minimization were performed with Protein Preparation Wizard of Schrödinger. The LigPrep module with OPLS3e force field was used to ionize and minimize the ligands. The preprocessed proteins and ligands were docked in the Ligand Docking module.

All of the MD simulations were performed using the Desmond software package. Firstly, the system was solvated, neutralized, and relaxed to avoid possible space collision. The force field uses OPLS3e, and the other options use the module default parameters. The box size is set to 10 Å . The temperature of all systems was controlled to be 300 K. The MD simulations were performed under the NVT ensemble for 100 ns.

Author contributions

Y.W., Y.Z. and Y.G. contributed equally to this manuscript. Y.W. and Y.Z. designed and synthesized the compounds, Y.G. analyzed the data and drafted the manuscript. X.J. and W.Z. performed the biological experiments, Z.P., S.Z., S.C. and J.G. performed the docking calculation and dynamic simulation, W.H., X.D. and J.C. conceived the study and helped to analyze the data.

Funding sources

The Leading Talent of “Ten Thousand Plan” - National High-Level Talents Special Support Plan; National Natural Science Foundation of China; Zhejiang Provincial Natural Science Foundation of China.

Declaration of competing interest

The authors declare that they have no known competing financial interests or personal relationships that could have appeared to influence the work reported in this paper.

Acknowledgements

We thank Jianyang Pan (Research and Service Center, College of Pharmaceutical Sciences, Zhejiang University) for performing NMR spectrometry for structure elucidation. This work was supported by grant from the Leading Talent of “Ten Thousand Plan” - National High-Level Talents Special Support Plan, the National Natural Science Foundation of China (81973172, 82003579), Zhejiang Provincial Natural Science Foundation (LR21H300003, LQ21H300005).

Appendix A. Supplementary data

Supplementary data to this article can be found online at

<https://doi.org/10.1016/j.ejmech.2021.113637>.

References

- [1] P. Sharma, J.P. Allison, The future of immune checkpoint therapy, *Science* 348 (2015) 56–61.
- [2] M. Mohme, S. Riethdorf, K. Pantel, Circulating and disseminated tumour cells - mechanisms of immune surveillance and escape, *Nat. Rev. Clin. Oncol.* 14 (2017) 155–167.
- [3] Y. Yang, Cancer immunotherapy: harnessing the immune system to battle cancer, *J. Clin. Invest.* 125 (2015) 3335–3337.
- [4] S.A. Rosenberg, Decade in review-cancer immunotherapy: entering the mainstream of cancer treatment, *Nat. Rev. Clin. Oncol.* 11 (2014) 630–632.
- [5] S.L. Topalian, J.M. Taube, R.A. Anders, D.M. Pardoll, Mechanism-driven biomarkers to guide immune checkpoint blockade in cancer therapy, *Nat. Rev. Canc.* 16 (2016) 275–287.
- [6] A. Kalbasi, A. Ribas, Tumour-intrinsic resistance to immune checkpoint blockade, *Nat. Rev. Immunol.* 20 (2020) 25–39.
- [7] C. Pan, H. Yang, Y. Lu, S. Hu, Y. Wu, Q. He, X. Dong, Recent advance of peptide-based molecules and nonpeptidic small-molecules modulating PD-1/PD-L1 protein-protein interaction or targeting PD-L1 protein degradation, *Eur. J. Med. Chem.* 213 (2021) 113170.
- [8] D.M. Pardoll, The blockade of immune checkpoints in cancer immunotherapy, *Nat. Rev. Canc.* 12 (2012) 252–264.
- [9] Q. Wu, L. Jiang, S.C. Li, Q.J. He, B. Yang, J. Cao, Small molecule inhibitors targeting the PD-1/PD-L1 signaling pathway, *Acta Pharmacol. Sin.* 42 (2021) 1–9.
- [10] N. Zhang, J. Tu, X. Wang, Q. Chu, Programmed cell death-1/programmed cell death ligand-1 checkpoint inhibitors: differences in mechanism of action, *Immunotherapy* 11 (2019) 429–441.
- [11] A. Swaika, W.A. Hammond, R.W. Joseph, Current state of anti-PD-L1 and anti-PD-1 agents in cancer therapy, *Mol. Immunol.* 67 (2015) 4–17.
- [12] T. Wang, X. Wu, C. Guo, K. Zhang, J. Xu, Z. Li, S. Jiang, Development of inhibitors of the programmed cell death-1/programmed cell death-ligand 1 signaling pathway, *J. Med. Chem.* 62 (2019) 1715–1730.
- [13] J. Tang, J.X. Yu, V.M. Hubbard-Lucey, S.T. Neftelinov, J.P. Hodge, Y. Lin, Trial watch: the clinical trial landscape for PD1/PDL1 immune checkpoint inhibitors, *Nat. Rev. Drug Discov.* 17 (2018) 854–855.
- [14] J. Xin Yu, J.P. Hodge, C. Oliva, S.T. Neftelinov, V.M. Hubbard-Lucey, J. Tang, Trends in clinical development for PD-1/PD-L1 inhibitors, *Nat. Rev. Drug Discov.* 19 (2020) 163–164.
- [15] S.L. Topalian, C.G. Drake, D.M. Pardoll, Immune checkpoint blockade: a common denominator approach to cancer therapy, *Canc. Cell* 27 (2015) 450–461.
- [16] R.J. Sullivan, K.T. Flaherty, Immunotherapy: anti-PD-1 therapies-a new first-line option in advanced melanoma, *Nat. Rev. Clin. Oncol.* 12 (2015) 625–626.
- [17] P. Khanna, N. Blais, P.O. Gaudreau, L. Corrales-Rodriguez, Immunotherapy comes of age in lung cancer, *Clin. Lung Canc.* 18 (2017) 13–22.
- [18] Y. Yan, L. Zhang, Y. Zuo, H. Qian, C. Liu, Immune checkpoint blockade in cancer immunotherapy: mechanisms, clinical outcomes, and safety profiles of PD-1/PD-L1 inhibitors, *Arch. Immunol. Ther. Exp.* 68 (2020) 36.
- [19] A. Constantinidou, C. Aliferis, D.T. Trafalis, Targeting Programmed Cell Death -1 (PD-1) and Ligand (PD-L1): a new era in cancer active immunotherapy, *Pharmacol. Ther.* 194 (2019) 84–106.
- [20] K.E. Beckermann, D.B. Johnson, J.A. Sosman, PD-1/PD-L1 blockade in renal cell cancer, *Expert Rev. Clin. Immunol.* 13 (2017) 77–84.
- [21] X. Lin, X. Lu, G. Luo, H. Xiang, Progress in PD-1/PD-L1 pathway inhibitors: from biomacromolecules to small molecules, *Eur. J. Med. Chem.* 186 (2020) 111876.
- [22] J. Zhang, Y. Zhang, B. Qu, H. Yang, S. Hu, X. Dong, If small molecules immunotherapy comes, can the prime be far behind? *Eur. J. Med. Chem.* 218 (2021) 113356.
- [23] B. Musielak, J. Kocik, L. Skalniak, K. Magiera-Mularz, D. Sala, M. Czub, M. Stec, M. Siedlar, T.A. Holak, J. Plewka, CA-170 - a potent small-molecule PD-L1 inhibitor or not? *Molecules* (2019) 24.
- [24] T. Chen, Q. Li, Z. Liu, Y. Chen, F. Feng, H. Sun, Peptide-based and small synthetic molecule inhibitors on PD-1/PD-L1 pathway: a new choice for immunotherapy? *Eur. J. Med. Chem.* 161 (2019) 378–398.
- [25] L.S. Chupak, X. Zheng, Compounds Useful as Immunomodulators, WO2015034820 A1, 2015.
- [26] L.S. Chupak, M. Ding, S.W. Martin, X. Zheng, P. Hewawasam, T.P. Connolly, N. Xu, K.-s. Yeung, J. Zhu, D.R. Langley, P.M. Scola, Compounds Useful as Immunomodulators, US 9850225 B2, 2017.
- [27] Z. Yu, L. Wu, W. Yao, Heterocyclic Compounds as Immunomodulators, vol. 18, US20180016260, January, 2018.
- [28] L. Wu, Z. Yu, F. Zhang, W. Yao, N-Phenyl-pyridine-2-carboxamide Derivatives and Their Use as PD-1/pd-L1 Protein/Protein Interaction Modulators, vol. 22, WO2017106634, June, 2017.
- [29] M. Qin, Q. Cao, X. Wu, C. Liu, S. Zheng, H. Xie, Y. Tian, J. Xie, Y. Zhao, Y. Hou, X. Zhang, B. Xu, H. Zhang, X. Wang, Discovery of the programmed cell death-1/programmed cell death-ligand 1 interaction inhibitors bearing an indoline scaffold, *Eur. J. Med. Chem.* 186 (2020) 111856.
- [30] J. Guo, L. Luo, Z. Wang, N. Hu, W. Wang, F. Xie, E. Liang, X. Yan, J. Xiao, S. Li, Design, synthesis, and biological evaluation of linear aliphatic amine-linked triaryl derivatives as potent small-molecule inhibitors of the programmed cell death-1/programmed cell death-ligand 1 interaction with promising antitumor effects in vivo, *J. Med. Chem.* 63 (2020) 13825–13850.
- [31] H. Chen, K. Wang, Y. Yang, X. Huang, X. Dai, Z. Feng, Design, synthesis, and structure-activity relationship of programmed cell death-1/programmed cell death-ligand 1 interaction inhibitors bearing a benzod[isothiazole scaffold, *Eur. J. Med. Chem.* 217 (2021) 113377.
- [32] L. Skalniak, K.M. Zak, K. Guzik, K. Magiera, B. Musielak, M. Pachota, B. Szlezak, J. Kocik, P. Grudnik, M. Tomala, S. Krzanik, K. Pyrc, A. Domling, G. Dubin, T.A. Holak, Small-molecule inhibitors of PD-1/PD-L1 immune checkpoint alleviate the PD-L1-induced exhaustion of T-cells, *Oncotarget* 8 (2017) 72167–72181.
- [33] K. Guzik, K.M. Zak, P. Grudnik, K. Magiera, B. Musielak, R. Torner, L. Skalniak, A. Domling, G. Dubin, T.A. Holak, Small-molecule inhibitors of the programmed cell death-1/programmed death-ligand 1 (PD-1/PD-L1) interaction via transiently induced protein states and dimerization of PD-L1, *J. Med. Chem.* 60 (2017) 5857–5867.
- [34] K.M. Zak, P. Grudnik, K. Guzik, B.J. Zieba, B. Musielak, A. Domling, G. Dubin, T.A. Holak, Structural basis for small molecule targeting of the programmed death ligand 1 (PD-L1), *Oncotarget* 7 (2016) 30323–30335.
- [35] S. Basu, J. Yang, B. Xu, K. Magiera-Mularz, L. Skalniak, B. Musielak, V. Kholodovych, T.A. Holak, L. Hu, Design, synthesis, evaluation, and structural studies of C2-symmetric small molecule inhibitors of programmed cell death-1/programmed death-ligand 1 protein-protein interaction, *J. Med. Chem.* 62 (2019) 7250–7263.
- [36] X. Yuan, H. Bu, J. Zhou, C.Y. Yang, H. Zhang, Recent advances of SHP2 inhibitors in cancer therapy: current development and clinical application, *J. Med. Chem.* 63 (2020) 11368–11396.
- [37] C. Krupka, P. Kufer, R. Kischel, G. Zugmaier, F.S. Lichtenegger, T. Kohnke, B. Vick, I. Jeremias, K.H. Metzler, T. Altmann, S. Schneider, M. Fiegl, K. Spiekermann, P.A. Bauerle, W. Hiddemann, G. Riethmuller, M. Subklewe, Blockade of the PD-1/PD-L1 axis augments lysis of AML cells by the CD33/CD3 BiTE antibody construct AMG 330: reversing a T-cell-induced immune escape mechanism, *Leukemia* 30 (2016) 484–491.
- [38] J. Qian, C. Wang, B. Wang, J. Yang, Y. Wang, F. Luo, J. Xu, C. Zhao, R. Liu, Y. Chu, The IFN-gamma/PD-L1 axis between T cells and tumor microenvironment: hints for glioma anti-PD-1/PD-L1 therapy, *J. Neuroinflammation* 15 (2018) 290.